ACS OMEGA

http://pubs.acs.org/journal/acsodf

Article

Surface-Modified Biobased Polymeric Nanoparticles for Dual Delivery of Doxorubicin and Gefitinib in Glioma Cell Lines

Ms Farheen, Md Habban Akhter,* Havagiray Chitme, Muath Suliman, Mariusz Jaremko, and Abdul-Hamid Emwas

Cite This: *ACS Omega* 2023, 8, 28165−28184

Read Online

ACCESS | Metrics & More | Article Recommendations

ABSTRACT: Glioma is a malignant form of brain cancer that is challenging to treat due to the progressive growth of glial cells. To target overexpressed folate receptors in glioma brain tumors, we designed and investigated doxorubicin−gefitinib nanoparticles (Dox-Gefit NPs) and folate conjugated Dox-Gefit NPs (Dox-Gefit NPs-F). Dox-Gefit NPs and Dox-Gefit NPs-F were characterized by multiple techniques including Fourier transform infrared spectroscopy (FT-IR), X-ray diffraction (XRD), differential scanning calorimetry (DSC), proton nuclear magnetic resonance (^{1}H NMR), and transmission electron microscopy (TEM). In vitro release profiles were measured at both physiological and tumor endosomal pH. The cytotoxicity of the Dox-Gefit NP formulations was measured against C6 and U87 glioma cell lines. A hemolysis assay was performed to investigate biocompatibility of the formulations, and distribution of the drugs in different organs was also estimated. The Dox-Gefit NPs and Dox-Gefit NPs-F were 109.45 ± 7.26 and 120.35 ± 3.65 nm in size and had surface charges of −18.0 ± 3.27 and −20.0 ± 8.23 mV, respectively. Dox-Gefit NPs and Dox-Gefit NPs-F significantly reduced the growth of U87 cells, with IC_{50} values of 9.9 and 3.2 μM. Similarly, growth of the C6 cell line was significantly reduced, with IC_{50} values of 8.43 and 3.31 μM after a 24 h incubation, in Dox-Gefit NPs and Dox-Gefit NPs-F, respectively. The percentage drug releases of Dox and Gefit from Dox-Gefit NPs at pH 7.4 were 60.87 ± 0.59 and 68.23 ± 0.1%, respectively. Similarly, at pH 5.4, Dox and Gefit releases from NPs were 70.87 ± 0.28 and 69.24 ± 0.12%, respectively. Biodistribution analysis revealed that more Dox and Gefit were present in the brain than in the other organs. The functionalized NPs inhibited the growth of glioma cells due to high drug concentrations in the brain. Folate conjugated NPs of Dox-Gefit could be a treatment option in glioma therapy.

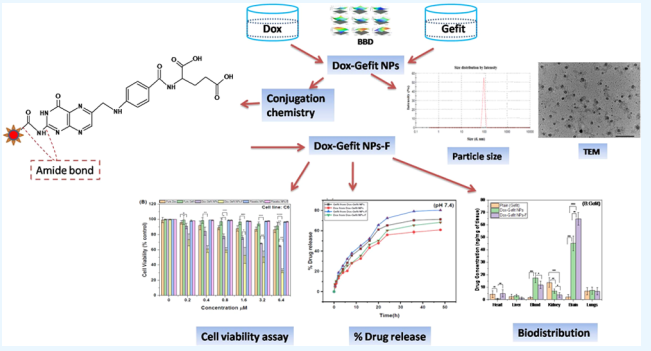

INTRODUCTION

Although recent decades have seen significant advances in cancer therapy, cancer is still a challenging health issue worldwide.[1] According to the American Cancer Society, 27.5 million new cases of cancer will occur by 2040. Primary brain tumors are among the most concerning malignant tumors since they are rarely curable and have a 5 year overall survival rate of only 35%.[2,3] Among brain diseases, brain malignancy is devastating and inadequately treated.[4] Adults with malignant brain tumors most frequently develop gliomas, which account for 80% of brain tumors.[5] FDA-recommended treatments include radiation therapy, surgical resection, and chemotherapy. The chemotherapy option is limited in glioma due to the high invasiveness and infiltrating nature of tumor cells into surrounding cells besides the blood−brain barrier (BBB). Tight junctions between endothelial cells and surrounding astrocytes control the passage of drugs from the systemic circulation into the brain. Besides the blood−brain barrier, a number of efflux transporters (such as breast cancer-resistance protein p-glycoprotein) are expressed in endothelial cells and further confine drug transport into the brain.[6] Considering this, the chemotherapeutics currently available for glioblastoma multiforme treatment have limited therapeutic efficacy and require high doses, leading to life-threatening toxicity. Surgery is successful for the complete removal of disease in some cases; often, relapse still occurs.[7,8] To overcome this issue, engineered nanoparticle-mediated drug delivery systems have been developed. These nanoparticle (NP) systems have been promising in preclinical glioma treatment studies, to administer single drugs or combinations via the intranasal route.[9] In particular, surface-tailored magnetic nanoparticles developed by

Received: March 1, 2023
Accepted: May 8, 2023
Published: July 26, 2023

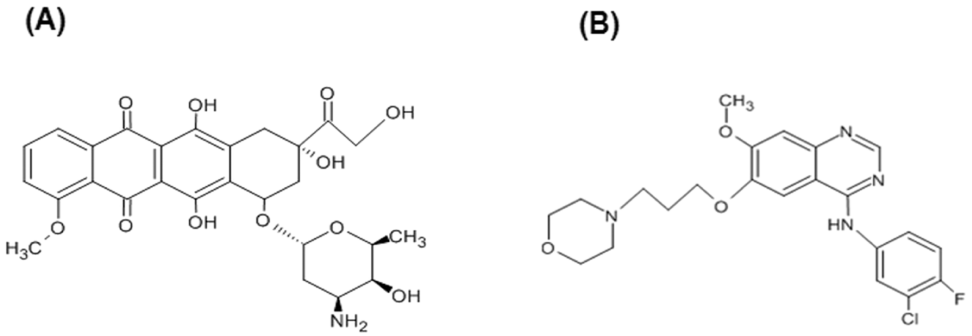

Figure 1. Structures of Dox (A) and Gefit (B).

Xu et al. have achieved high drug penetration and therapeutic efficacy in glioma.[10]

Biobased polymers have recently gained wider attention as nanocomposites with wide-ranging features including biodegradability, biocompatibility, stability, flexibility, low immunogenicity, renewability, and bioresorbability.[11] Significant work has established polysaccharide-based biopolymers for drug delivery and biomedical applications, replacing synthetic nonmaterials.[12] Biopolymers can be easily broken down by naturally occurring microorganisms and enzymes, producing organic byproducts that are not detrimental to biological systems.[13] Biopolymer-based nanocarriers may improve drug release and access to specific target sites over extended periods, thus improving the bioavailability of encapsulated drugs. Biobased polymers obtained from the bark of *Cinnamomum Zeylanicum* have promising drug encapsulation efficiency, and their surfaces may also be modified.[14]

The emergence of nanotechnology has made drug delivery into the brain easier when combined with advances in drug delivery technology and targeting.[15] The development of novel nanocarriers has allowed for the selective and targeted delivery of therapeutic agents to specific cells, tissues, and organs while avoiding healthy tissues.[16] The surface of natural polymers can be modified, encapsulating cargo for site-specific polymeric delivery. Natural polymers have distinctive physicochemical qualities that allow them to be used as drug carriers to the brain. These properties include biodegradability, biocompatibility, reduced toxicity, and special functionality such as a flexible surface and plasticity.[17,18]

Targeted drug delivery to tumors unlocks new possibilities for a vast number of chemotherapies.[19] Tumor-targeted strategies that have evolved recently include cell-based targeted therapies, gene therapy, immunotherapy, and viral therapy. Active drug targeting relies on NPs (carrying cargos) to hit targets with limited off-target release. Targeted NPs take advantage of a unique interaction between ligands conjugated to the NPs and receptors expressed on the surface of tumor target cells. Versatile NPs may improve controlled release for a desired time and maintain drug stability. Ligated NPs may be a promising system for precise drug delivery.[20−24]

The folate receptor is a cysteine-rich glycoprotein that binds folic acid and is overexpressed in the glioma.[25] The folate-decorated nanocarrier has a high affinity to binding with the folate receptor, which leads to cellular internalization through the formation of endosomes via an endocytic pathway in glioma cells. The folate-grafted nanocarrier after cell internalization unbinds in the acidic pH of the tumor microenvironment, followed by the receptor recycling back to the cell surface and subsequently drug being released into the cytosol.[26,27]

Combinatorial therapy both diminishes the development of cancer-resistant cells and synergistically improves the therapeutic efficacy of targeted molecules.[28] The simultaneous release of Gefit (EGFR inhibitor) may increase the level of DNA damage caused by Dox due to better sensitization.[29] The simultaneous localization of medications at an effective dose is a major factor in achieving synergistic effects.[30]

Doxorubicin is one of the most frequently used chemotherapeutics, used to treat a variety of solid tumors including in the brain.[31] It is an anthracyclic group antibiotic used as an antineoplastic drug.[32] It works via a variety of mechanisms including DNA intercalation, dislocation of topoisomerase II, and free radical generation, all of which result in cellular damage. A cumulative dose of over 550 mg/m^2 Dox may cause cardiac failure and therefore can be life-threatening at too high a dose.[33]

Gefit is an EGFR−tyrosine kinase inhibitor approved by the FDA for breast and lung cancer treatment. The antitumor effects of Gefit are increased in combination with chemotherapy.[34−36] The chemical structures of Dox and Gefit are shown in Figure 1A,B. Lakkadwala and associates developed transferrin-modified liposomes for Dox and Erlotinib for targeting into glioma cells. In vitro profiles showed higher translocation of chemotherapeutics in tumors cells indicated by the in vitro brain tumor model.[37]

Surface-functionalized NPs may bind more effectively with overexpressed cell surface receptors on glioma cells, with better cellular uptake and drug internalization in tumor cells. Here, we develop Dox-Gefit-loaded biopolymeric NPs and folate-decorated biopolymeric NPs via conjugation chemistry for receptor-mediated targeting of brain cancer. We evaluated numerous physicochemical characteristics of these formulations in vitro, including particle size and surface charge, and evaluated their effects on glioma cell lines, such as cytotoxicity.

MATERIALS AND METHODS

Gefitinib (M_w = 446 g/mole, purity ≥95%) was a gift from Natco Pharma Pvt. Ltd. (Dehradun, India). Dox was a gift from Neon Laboratories Pvt. Ltd. (Ghaziabad, India). Cinnamon biopolymer was purchased from Shree Ram Overseas (New Delhi, India). Poly(vinyl alcohol) (PVA) was from Sisco Research Laboratory Pvt. Ltd. (Mumbai, India). The cross-linking agents EDC [1-(3 dimethylaminopropyl)-3-ethyl carbodiimide hydrochloride] and sulfo-NHS [*N*-hydroxysuccinimide] were from Sisco Research Laboratories Pvt. Ltd. (Mumbai, India). The organic solvent dimethyl sulfoxide (DMSO) was from Merck Pvt. Ltd. (Mumbai, India). Acetone, deionized water, and HPLC-grade water were obtained from SD Fine Chem Pvt. Ltd. (Mumbai, India). Other chemicals and reagents were of analytical grade.

https://doi.org/10.1021/acsomega.3c01375
ACS Omega 2023, 8, 28165−28184

Cytotoxicity Studies. *Materials.* Culture media, penicillin streptomycin, MTT ((4,5-dimethylthiazol-2yl)-2,5-diphenyl tetrazolium bromide), fetal bovine serum (FBS), and Dulbecco's modified Eagle's medium (DMEM) were purchased from Himedia India (Gibco). The phosphate-buffered saline (PBS) was obtained from Himedia, India (Gibco). The NCCS in Pune, India, provided C6 and U87 cell lines. Cells were kept at 37 °C and 5% CO_2 in a humidified CO_2 incubator for continuous growth.

Experimental Design for Formulation Optimization. To produce an optimal formulation, the Box−Behnken experimental design was used. Three distinct variables were chosen: polymer concentration (conc.) (A), surfactant conc. (B), and sonication time (C), with levels either low (−1), intermediate (0), or high (+1) (Table 1). The concentration of variables selected was based on preliminary investigation.[38] One-way ANOVA was used to calculate significant values for a model of good fit in producing the final formulation. The optimized composition of the formulation was produced by measuring the particle size (minimize), PDI (minimize), and % drug release (maximize). The point prediction technique was followed to conclude the formulation.

Table 1. Nanoparticle Development Using the Box−Behnken Response Surface Design[a]

	levels		
independent variables (factors)	low (−1)	intermediate (0)	high (+1)
A: polymer conc. (%)	1.00	2.50	4.00
B: surfactant conc. (%)	1.00	2.00	3.00
C: sonication time (min)	5.00	10.00	15.00
dependent variables (responses)		desirability constraints	
R^1: particle size (nm)		minimize	
R^2: PDI		minimize	
R^3: drug release (%)		maximize	

[a]The table shows the levels implemented for different independent variables and desirability constraints.

PREPARATION OF DOX-GEFIT LOADED NPS

The Dox-Gefit loaded biopolymeric NPs were prepared using the double-emulsion solvent evaporation technique.[39] Gefit solution was prepared in the organic phase (1 mg/mL), Dox was added in the aqueous phase (5 μg/mL), and an aqueous biopolymeric solution of 5 mL was used at a concentration of 21.9 mg/mL. 3 mL of aqueous PVA was used as a surfactant solution, prepared at a concentration of 17.3 mg/mL. First, Gefit (1 mg/mL) and Dox solution (5 μg/mL) together were transferred slowly using an injectable needle into the biopolymeric solution (21.9 mg/mL) and emulsified using PVA and a probe sonicator (Hielscher ultrasonicator, Berlin, Germany) (2 min, 30 KHz power, 50 W, one cycle). The resulting solution formed the Dox-Gefit loaded primary emulsion (o/w). Next, the primary emulsion was transferred into an aqueous surfactant solution (17.3 mg/mL) slowly using an injection needle at the rate of 0.5 mL/min and emulsified for 8.6 min using a probe sonicator (30 KHz power, 80 W, one cycle). The resulting secondary emulsion comprised NPs. Subsequently, the preparation was stirred magnetically at 1000 rpm for 4 h at ambient temperature to allow the evaporation of the organic phase. Then, the preparation was kept open overnight to harden and obtain dry NPs. Further, the NPs were ultracentrifuged at 15,000 rpm (OptimaTE-80K Ultracentrifuge) for 30 min and washed thrice to obtain NPs free from unentrapped drugs as well as free biopolymers. Next, the Dox-Gefit loaded NPs were redispersed in water and lyophilized to dryness for future characterization.

SURFACE MODIFICATION OF DOX-GEFIT NPS

The developed Dox-Gefit NPs were redispersed in Eppendorf tubes containing water, at a concentration of 10 mg/mL. 0.1% w/v 1-(3 dimethyl amino propyl)-3-ethyl carbodiimide hydrochloride (EDC.HCl) was added. It was then vortexed before adding *N*-hydroxysuccinimide [Sulfo-NHS, 0.05% w/v] and incubated in a biological shaker in the dark for 5 h to activate the functional carboxylic group on the biopolymeric surface. During incubation, an unstable intermediate reaction product was formed between the NPs, with EDC.HCL as the cross-linker. This further reacted with sulfo-NHS, resulting in a stable ester. In the subsequent step, the surface-activated NPs were

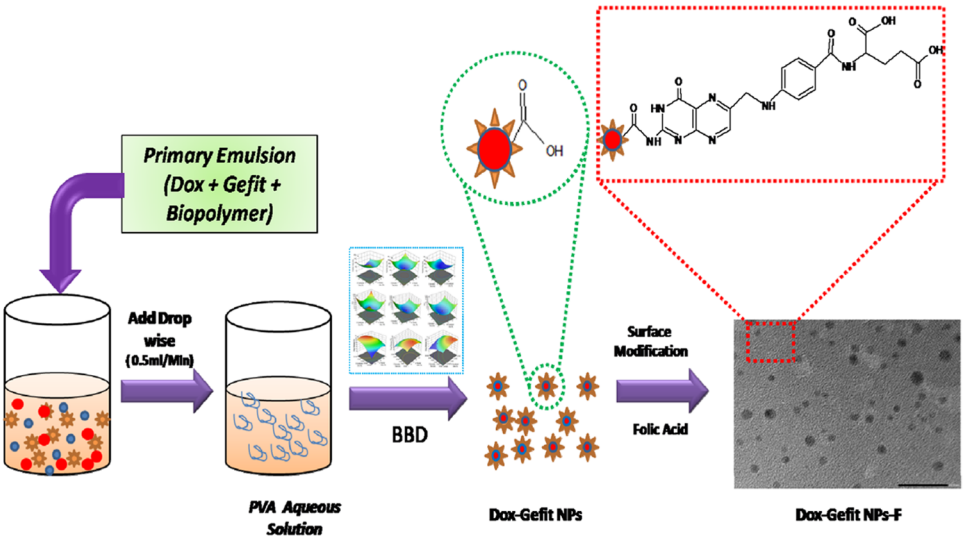

Figure 2. Schematic representation of Dox-Gefit NPs-F preparation.

https://doi.org/10.1021/acsomega.3c01375
ACS Omega 2023, 8, 28165−28184

centrifuged at 15,000 rpm for 30 min and washed in PBS pH 7.4 after discarding the supernatant. Further, NPs were dried and redispersed in 2 mL of PBS. Next, 0.1% w/v folic acid was prepared by dissolving 10 mg of folic acid in 10 mL of sodium hydroxide (1 mg/mL). 2 mL of folic acid was added to the NPs and incubated at ambient temperature in a biological shaker. Further, the folate coupled NPs (Dox-Gefit NPs-F) were centrifuged at 15,000 rpm for 30 min, and then, the supernatant was removed containing a fraction of free EDC, free sulfo-NHS, and free folic acid and the Dox-Gefit NPs-F suspension was obtained, which was washed in a buffer. Dox-Gefit NPs-F (10 mg/mL) was redispersed in deionized water. One drop of 0.25 M ethanolamine was added and then incubated for 30 min to block unreacted sites on the NPs and washed with Milli Q water. The Dox-Gefit NPs-F was then lyophilized for further use. The technique for the preparation of Dox-Gefit NPs and their surface modification with folate is shown in Figure 2.

Characterization of Dox- Gefit NPs and Dox-Gefit NPs-F. *Particle Size Analysis.* The particle size distribution and particle diameter were analyzed as a *z*-average in the NP formulation using a Zetasizer 1000 HS (Malvern Instruments, U.K.). NPs were dispersed in HPLC-grade water (0.5 mg/mL) and bath-sonicated, and then, sizing analysis was computed in triplicate ($n = 3$).

Drug Entrapment Efficiency. The amount of unentrapped Gefit and Dox in the NP and Dox-Gefit NP-F samples was evaluated by quantifying their concentration in the supernatant using a UV−visible spectrophotometer at λ_{max} values of 331 and 480 nm. The supernatant was obtained after centrifuging the samples at a speed of 15,000 rpm, at 4 °C for 30 min (C24, REMI Refrigerated Centrifuge, Mumbai, India). The % entrapment efficiency of drugs in the NPs and functionalized NPs was estimated using the following equation

$$\%\ \text{entrapment efficiency} = (\text{total drug concentration} - \text{supernatant drug})/(\text{total amount of drug}) \times 100$$

High-Resolution Transmission Electron Microscopy (HR-TEM). The particle shape and surface morphology of the NPs were studied by JEOL, JEM 2100 Plus (Japan), which was operated at 80−200 kV, ultrahigh resolution (UHR). The diluted NPs (0.5 mg/mL) were spread over a permeable film grid and dried, and images were observed and captured at 80−200 kV.

Fourier Transform Infrared Spectroscopy (FT-IR). FT-IR spectra of pure Dox, Gefit, cinnamon biopolymer, PVA, Dox-Gefit NPs, and Dox-Gefit NPs-F were taken using FT-IR (Tensor 37, Bruker). A sample of weight 5 mg was directly placed into the beam light path, and the spectra of different components under study were recorded in the scanning range of 4000−400 cm^{-1}.

Differential Scanning Calorimetry (DSC). DSC was used to determine the melting point, the physical state of the drug Dox, Gefit, biopolymer, PVA, Dox-Gefit NPs, and Dox-Gefit NPs-F by using DSC (LABSYS EVO 1150 °C DSC131 EVO analyzer, Setaram Instrumentation, France).

X-ray Diffraction (XRD). XRD analyses were performed with a PAN analytical X'pert PRO (The Netherlands), working at 40 kV, 30 mA, and 2θ angle ranges (0−80°) applying monochromatic CuKa radiation ($k = 1.5406$ Å).

Proton Nuclear Magnetic Resonance (^1H NMR). The ^1H NMR spectra of Dox-Gefit NPs-F were acquired on a Bruker Avance-II (Switzerland) at 400 MHz. Chemical shifts were reported in ppm for structural elucidation to confirm folate conjugation to the activated surface of the biopolymer.[40]

In Vitro Release Studies. The % drug release from the drug delivery system was determined at physiological pH 7.4 and pH 5.4 (simulating intracellular endosomal pH) at the temperature of 37 ± 0.5 °C for 48 h. 20 mg of each formulation (such as Dox-Gefit loaded NPs and Dox) was transferred into a dialysis bag (Mol. wt cutoff = 6−8 kDa), and the ends were tightened. The dialysis bag was then immersed in 100 mL of PBS at either pH 7.4 or pH 5.4 and at 37 ± 0.5 °C and continuously shaken at 50 rpm. Several 2 mL samples were withdrawn at programmed intervals of 0, 0.5, 1, 2, 4, 6, 8, 12, 16, 20, 24, 36, and 48 h, and the same volume of sample was replaced with a buffer at pH 7.4 or pH 5.4. The collected samples were examined at λ_{max} values of 331 and 480 nm using a UV−visible spectrophotometer. % drug released from NPs was obtained and fitted to various kinetic models to screen out a model of good fit and a suggested mechanism of drug release from the biopolymeric surface. The % drug released from NPs was estimated using the following equation

$$\%\ \text{drug release} = (\text{amount of drug released at interval})/(\text{total amount of drug}) \times 100$$

Hemolytic Study. The hemolysis assay was performed to examine the compatibility of biopolymeric NPs in contact with blood, with modifications as described by Augustine et al.[41] Blood was collected in EDTA-coated tubes from adult rats and centrifuged at 2000 rpm for 10 min to separate RBC cells. Triton-X-100 and normal saline were positive and negative controls in this assay, respectively. To execute the assay, placebo NPs, Dox-Gefit NPs, or Dox-Gefit NPs-F were tested with blood by gradually increasing their quantity, starting with 1.5, 3, and 6 mg. Each concentration of sample was dispersed in 500 μL of saline and incubated with diluted blood at 37 ± 0.5 °C for 1 h. Subsequently, the samples were centrifuged at 1500 rpm for 5 min. The supernatant containing released hemoglobin was examined at 541 nm using a UV−visible spectrophotometer. The following formula was used to determine the % hemolysis

$$\%\ \text{hemolysis} = (\text{sample absorbance} - \text{negative control absorbance})/\text{positive control absorbance} \times 100$$

Cytotoxicity Studies and Determination of the Combination Index (CI). The cytotoxicity of Dox-Gefit-NPs or Dox-Gefit-NPs-Fs was investigated with the glioma cell lines U87 (ATCC, HTB14) and C6 (ATCC, CCL107) using a calorimetric MTT assay that measures cell viability.[42] Cell lines were added to 96-well plates containing the DMEM medium at a concentration of 10^6 cells/well and subsequently incubated overnight night at 37 °C in a humidified atmosphere and 5% v/v CO_2 containing air (5% v/v).[43] After cell attachment, wells were treated with varying concentrations of 0.2, 0.4, 0.8, 1.6, 3.2, and 6.4 μM Dox-Gefit-NPs and Dox-Gefit-NPs-F and incubated for 24 h. After completion of the treatment, the media was discarded carefully, and the cells were incubated with 100 μL of MTT for 3 h. Further, 150 μL of DMSO was transferred into each well and incubated for 10 min, which resulted in a reduction of the yellow

https://doi.org/10.1021/acsomega.3c01375
ACS Omega 2023, 8, 28165−28184

Table 2. Box−Behnken Response Surface Design Produced 17 Runs for the Optimization of Manufactured Nanoparticles

runs	factor 2 A: polymer conc. (% w/v)	factor 1 B: surfactant conc. (% w/v)	factor 3 C: sonication time (min)	response 1 particle size (nm)	response 2 PDI	response 3% drug release
1	2.5	2	12.5	92	0.103	82
2	2.5	1	20	300	0.183	50
3	2.5	3	5	189	0.213	50
4	1	3	12.5	220	0.236	70
5	1	2	5	350	0.196	60
6	2.5	3	20	160	0.198	65
7	2.5	2	12.5	90	0.101	82
8	2.5	2	12.5	98	0.106	85
9	2.5	2	12.5	99	0.109	82
10	4	2	5	318	0.215	50
11	2.5	2	12.5	92	0.107	82
12	2.5	1	5	310	0.186	60
13	1	2	20	312	0.216	60
14	1	1	12.5	320	0.24	50
15	4	2	20	310	0.187	50
16	4	1	12.5	320	0.214	60
17	4	3	12.5	180	0.240	40

color MTT dye into formazan crystals (purple-colored). Next, the optical density was estimated using a microplate reader at 570 nm. Three replicates of each experiment were carried out (n = 3). Untreated cells were taken as the control group (100% cell viability), and the IC_{50} of the cells was determined. IC50 is the drug concentration that slows down cell growth by 50% compared to the control. It was calculated by using regression of the cell viability data. The combination index (CI) was determined to measure the combination effect for codelivery of Dox and Gefit. It is based on the IC50 value of the drugs achieved on the MTT assay and values calculated using the following formula. It was noted that if CI > 1, it indicates an antagonistic effect; if CI = 1, it indicates an additive effect; and if CI < 1, it means a synergistic effect.

The following formula was used to calculate the cell viability (%) as mean viability (%) and standard deviation (SD) (n = 3). Percent cell viability = OD treated/OD controlled × 100

$$\mathrm{CI} = \frac{IC_{50}(A+B)}{IC_{50}(A)} + \frac{IC_{50}(A+B)}{IC_{50}(B)}$$

where IC_{50} (A), IC_{50} (B), and IC_{50} $(A + B)$ indicate the IC_{50} values of Dox, Gefit, and the combination drug obtained in the MTT assay, respectively.

Biodistribution Studies. Animals were placed in the animal house prior to the testing and preserved in a polymeric cage as per the ethical guidelines of the animal. The animals were kept at room temperature with a 12 h light/dark cycle with nourishing water ad libitum. The protocol and procedures were approved by the Institutional Animal Ethics Committee (IAEC) guidelines of DIT University, Dehradun, Uttrakhand, India (Ref no. DITU/IAEC/21-22/07-05). A single dose each of pure Gefit, pure Dox, Dox-Gefit-NPs, and Dox-Gefit-NPs-F were given in a volume of 20 μL via the nose once a day for 14 days in four groups of male Wistar rats (n = 3). The liver, kidney, heart, blood, lungs, and brain were removed from each group (n = 3) after 24 h of the last dose. The tissue was dried with tissue paper, weighed, and homogenized in an ice-cold 1 mL sodium chloride solution per gram of tissue. Thereafter, the samples were separated and kept at −20 °C until analysis. The Dox and Gefit contents were analyzed by HPLC.

Stability Study. Samples were kept in a stability chamber at a temperature of 25 ± 2 °C, 65 ± 5% RH, and at 40 ± 2 °C, 75 ± 5% RH, for 90 days. Evaluations were conducted at intervals of 0, 30, 60, and 90 days.[44,45]

Fetal Bovine Serum (FBS) Stability of Dox-Gefit-NPs-F. The lyophilized sample of Dox-Gefit NPs-F weighing ∼1 mg was redispersed in a PBS of pH 7.4. To assess the nanodrug stability of Dox-Gefit NPs-F, it was incubated with 10% fetal bovine serum (FBS) at 37 °C to interpret the impact of serum protein in the medium on the formation of protein layering around functional NPs. The Dox-Gefit NPs-F dispersion was added into 10% FBS solution in the ratio of 1:1; the resulting serum concentration was adjusted to 50% v/v using the formulation. Thereafter, the solution mixture was incubated in a water bath incubator at 37 °C for 24 h.[46] The mean particle size (nm) and ζ potential (mV) were measured post incubation at predetermined time points (0.5, 1, 4, 6, 12, and 24 h) by withdrawing 1 mL of samples. At different intervals of 0.5, 1, 4, and 6 h, the ultraviolet scan of the sample was performed to estimate the variation in absorbance in relation to the incubation time using a UV spectrophotometer.

Statistical Analysis. One-way analysis of variance (ANOVA), with significant values of $p < 0.05$, was utilized for all of the reported analysis accompanied by a Tukey−Kramer analysis using GraphPad prism (version 7). All of the results were provided as a mean of standard deviation, and each experiment was carried out in triplicate.

RESULTS

Selection of Optimized Dox-Gefit NPs. A Box−Behnken design was used to generate 17 experimental runs. Three factors were used with three levels (low (−1), intermediate (0), and high (+1)). The expert design is economic and requires less time to optimize the formulation and, therefore, it was adopted in this study (Version 10; Stat Ease Inc., Minneapolis, MN). The listings of independent variables are shown in Table 1. The various experimental runs were generated by software, based on chosen variables such as polymer concentration (A), surfactant

https://doi.org/10.1021/acsomega.3c01375
ACS Omega 2023, 8, 28165−28184

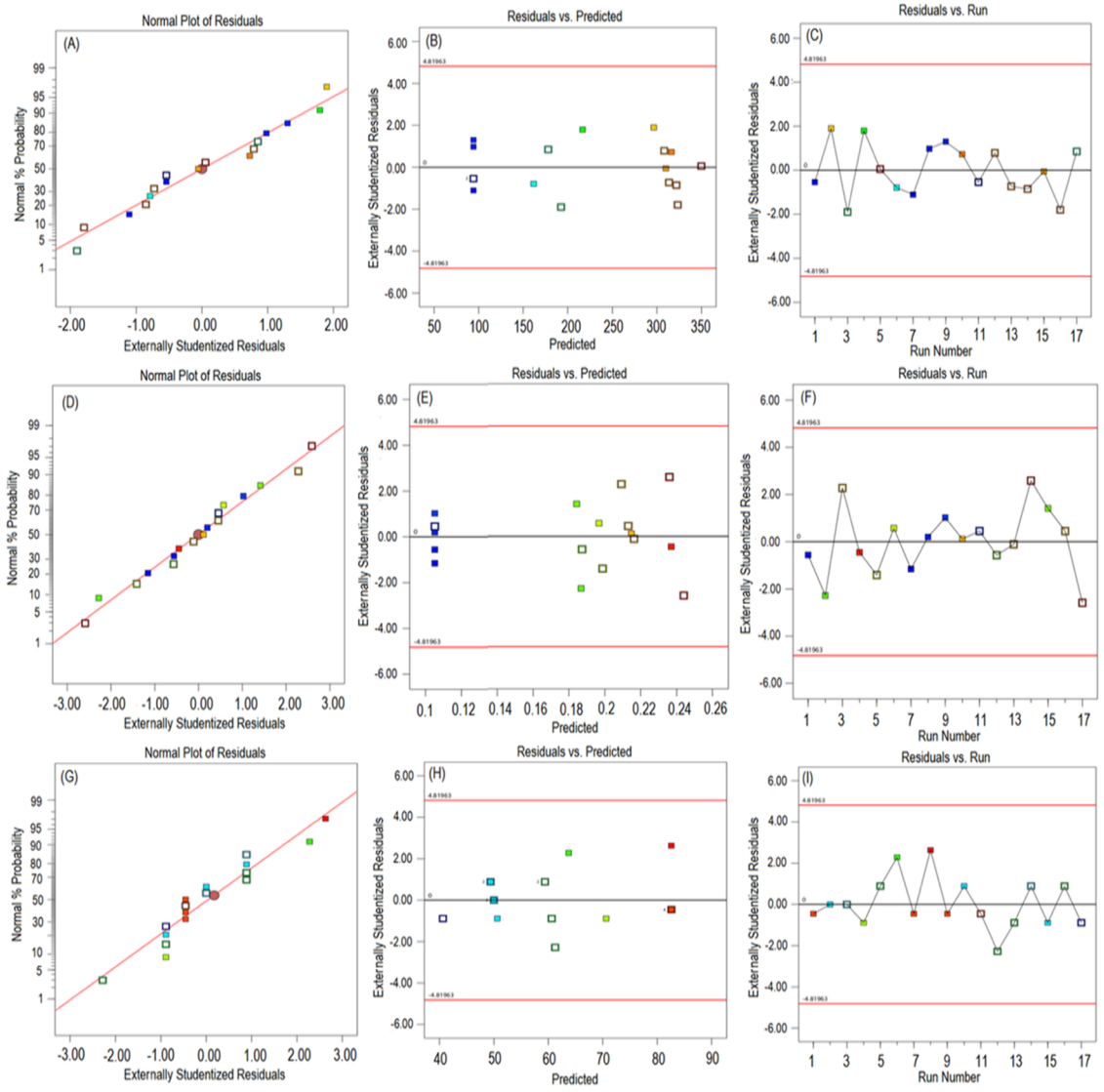

Figure 3. NP diagnostic plots. (A) Normal % probability plot of particle size. (B) Externally studentized residuals vs. predicted plot of particle size. (C) Externally studentized residuals vs runs of particle size. (D) Normal % probability plot of PDI. (E) Externally studentized residuals vs predicted plot of PDI. (F) Externally studentized residuals vs run of PDI. (G) Normal % probability plot of % drug release. (H) Externally studentized residuals vs. predicted plot of % drug release. (I) Externally studentized residuals vs run of % drug release.

concentration (B), and sonication time (C), as shown in Table 2. A diagnostic plot of NPs is shown in Figure 3, showing properties such as normal % probability, externally studentized residuals vs. predicted plot of particle size, PDI, and % drug release. A three-dimensional response surface morphology is shown in Figure 4, indicating the impact of independent variables, viz., polymer, surfactant, and sonication time, on dependent variables, viz., particle size, PDI, and % drug release.[39] The high and low levels of independent variables were established based on the preliminary laboratory observation for developing formulation. A trial and error method of selecting the excipients in the formulation assured a robust and consistent formulation.[47] The best-fitting model was found to be quadratic with the highest estimated value of coefficient of correlation (R^2)~1.

The NP particle size ranged from 90 to 350 nm (Table 2). The coefficient of correlation in a quadratic model of particle size gave an adjusted R^2 value of 0.9982 and a predicted R^2 value of 0.9929. The % drug release from the NPs ranged between 40 and 85% represented by a quadratic model with an adjusted R^2 value of 0.9937 and a predicted R^2 value of 0.9691. The NP PDI value ranged from 0.101 to 0.240 with an adjusted R^2 value of 0.9909 and a predicted R^2 value of 0.9672. The mathematical quadratic equations drawn from the experimental design for calculation of particle size, PDI, and % drug release are shown below.

$$\begin{aligned}\text{particle size} = {} & +94.20 - 9.25 \times A - 62.62 \times B \\ & - 10.63 \times C - 10.00 \times A \times B \\ & + 7.50 \times A \times C - 4.75 \times B \times C \\ & + 124.28 \times A^2 + 41.52 \times B^2 \\ & + 104.03 \times C^2\end{aligned}$$

$$\begin{aligned}\text{PDI} = {} & +0.1052 - 0.0040 \times A + 0.0080 \times B \\ & - 0.0033 \times C + 0.0075 \times A \times B \\ & - 0.0120 \times A \times C - 0.0030 \times B \times C \\ & + 0.0679 \times A^2 + 0.0594 \times B^2 + 0.0304 \times C^2\end{aligned}$$

https://doi.org/10.1021/acsomega.3c01375
ACS Omega 2023, 8, 28165−28184

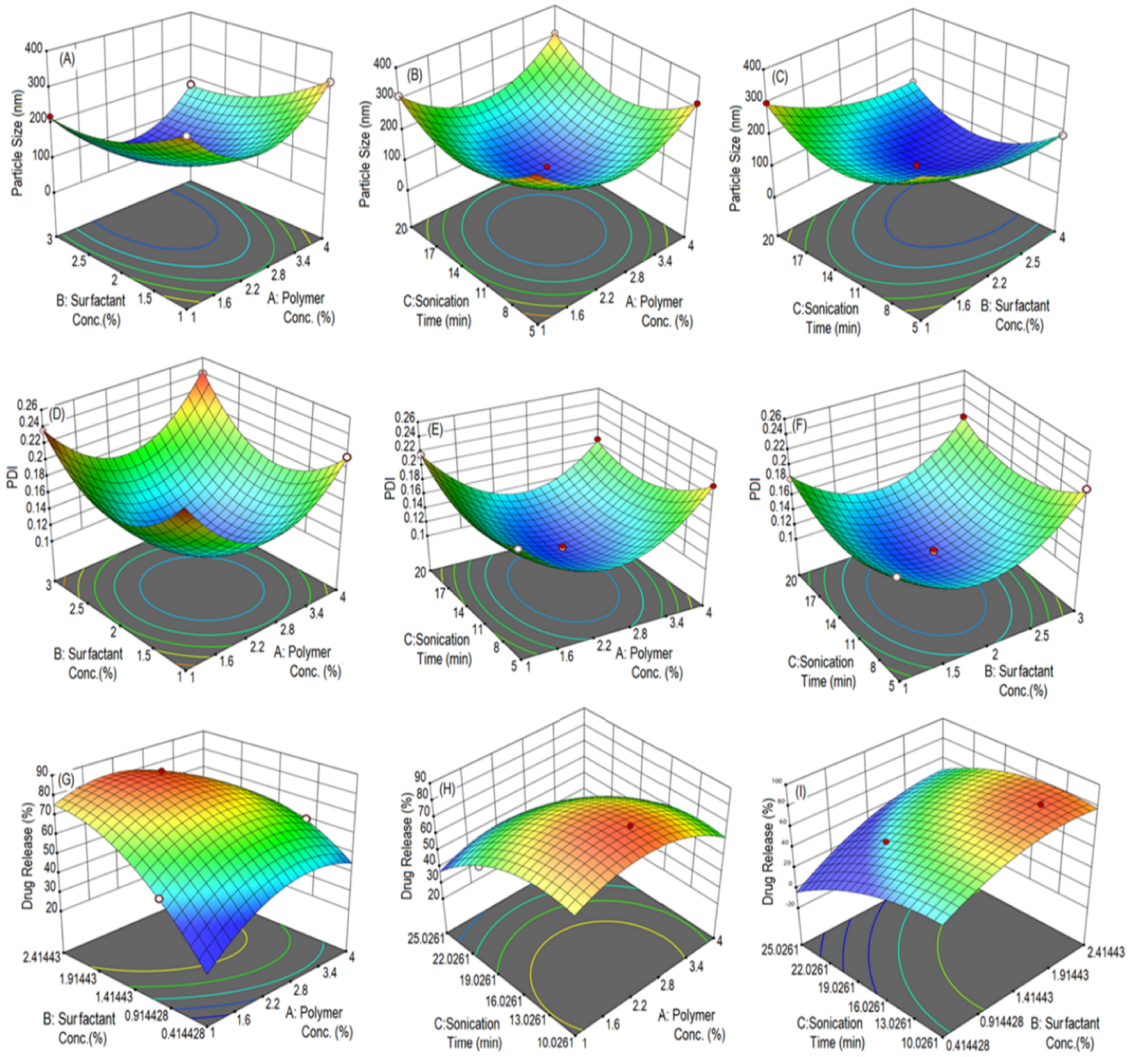

Figure 4. 3-D response surface plots. (A−I) Comparative effective surfactant conc., polymer conc., and sonication time on particle size (A−C), PDI (D−F), and % drug release (G−I).

$$\%\ \text{drug release} = +82.60 - 5.00 \times A + 0.6250 \times B + 0.6250 \times C - 10.00 \times A \times B + 6.25 \times B \times C - 14.43 \times A^2 - 13.17 \times B^2 - 13.18 \times C^2$$

Validation of Optimum Formulation. Among the optimal solutions for formulation, the validation of a few predicted experiments was investigated, and the findings led to an agreement with the predicted values. The optimum formulation was finalized using numerical optimization tools, keeping the criteria of particle size (minimize), PDI (minimize), and % drug release (maximize). The developed optimized formula was robust and stable with a desirability value of 0.851. The optimum composition of the developed Dox-Gift NPs was a biopolymer conc. of 2.19% w/v, a surfactant conc. of 1.73% w/v, and a sonication time of 8.6 min. The software-predicted values for the dependent variables were identified as follows: particle size, 116.18 nm; PDI, 0.12; and % drug release, 78.2%. Moreover, the experimental values for particle size were 109.45 ± 7.2 nm; PDI, 0.10; and % drug release, 70.04%.

Characterization of Dox-Gefit NPs and Dox-Gefit NPs-F. *Particle Size and ζ Potential.* The measured particle sizes and ζ potentials of Dox-Gift NPs and Dox-Gefit NPs-F are shown in Figure 5A,B. The particle sizes of Dox-Gefit-NPs and Dox-Gefit-NPs-F were 109.45 ± 7.26 and 120.35 ± 3.65 nm, respectively. For the surface-functionalized NPs, the particle size was slightly larger than that of bare NPs, perhaps due to ligation of folate onto the surface of Dox-Gefit-NPs during functionalization. The TEM images of Dox-Gefit-NPs and Dox-Gefit-NPs-F (Figure 6A,B) indicate that particles were uniform and consistent and in agreement with the size prevailed by the Malvern Zetasizer. The ζ potentials of Dox-Gefit NPs and Dox-Gefit NPs-F were −18.0 ± 3.27 and −20.0 ± 8.23 mV, respectively, as shown in Figure 5C,D. The entrapment efficiencies of Gefit and Dox were 82 ± 4.2 and 77 ± 5.6%, respectively, for Dox-Gefit NPs and 83 ± 2.9 and 78 ± 6.67%, respectively, for Dox-Gefit NPs-F. PDI values of Dox-Gefit NPs and Dox-Gefit NPs-F were 0.107 and 0.110, respectively. The predicted particle size of the optimized NPs was 116.18 nm, while the experimental value of the particle size was determined to be 109.45 ± 7.26 nm. Further, the predicted PDI values were 0.121 and 0.107 for the experimental and predicted values, respectively. The predicted and experimental values for % drug release were 78.27 and 70.04%, respectively, as shown in Table 3.

https://doi.org/10.1021/acsomega.3c01375
ACS Omega 2023, 8, 28165−28184

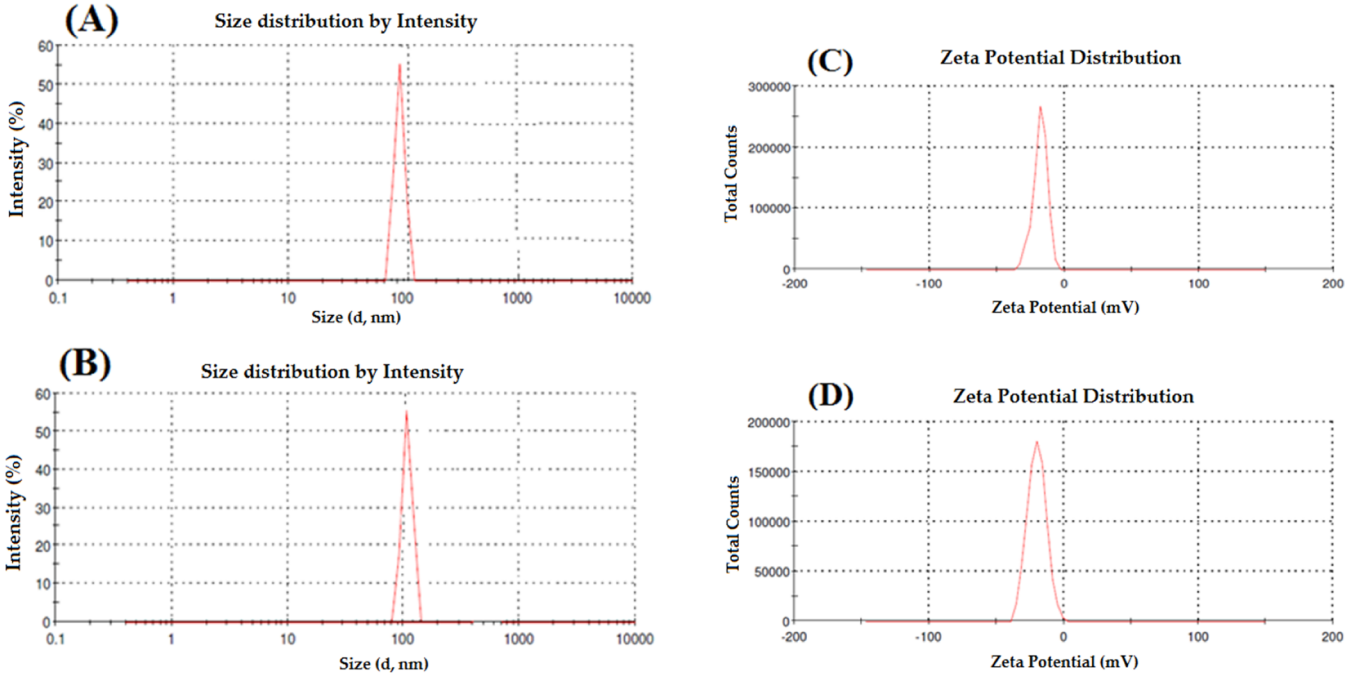

Figure 5. Dox-Gefit NP and Dox-Gefit NPs-F particle size and ζ potential. (A) Dox-Gefit NP size distribution. (B) Dox-Gefit NPs-F size distribution. (C) ζ Potential of Dox-Gefit NPs. (D) ζ Potential of Dox-Gefit NPs-F.

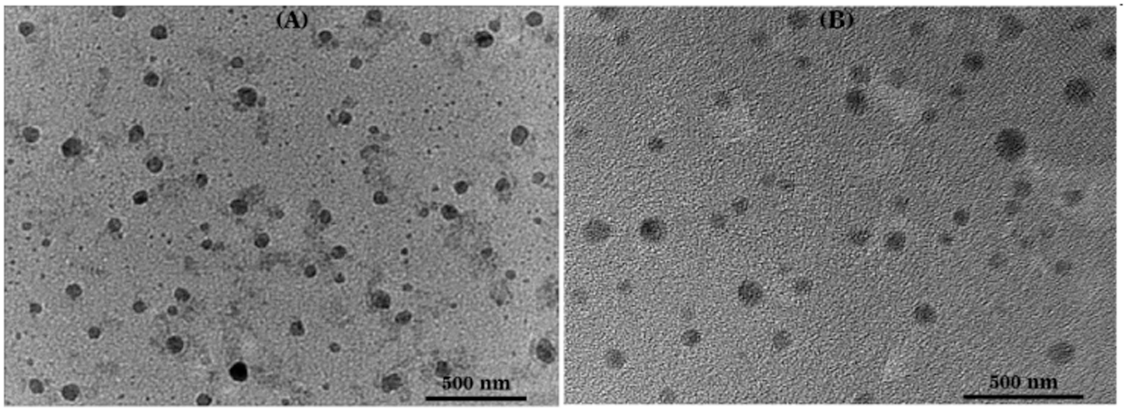

Figure 6. Transmission electron microscopy of Dox-Erlo NPs (A) and Dox-Erlo NPs-F (B).

Table 3. Optimized Composition of Dox-Gefit NPs with Predicted and Experimental Values

variables	optimum composition	responses	predicted value	experimental value
A	2.19%w/v	R^1	116.18 nm	109.45 ± 7.26 nm
B	1.73% w/v	R^2	0.121	0.107
C	8.6 min	R^3	78.27%	70.04%

DSC Analysis. The DSC spectra of pure Dox, Gefit, cinnamon biopolymer, PVA, Dox-Gefit NPs, and Dox-Gefit NPs-F are shown in Figure 7A−F. The DSC thermogram of Gefit showed a distinct endothermic peak at 194.181 °C. DSC and Dox peaks were obtained at a melting point of 170 °C and at 222.674 °C, respectively. The cinnamon biopolymer showed a flat endothermic peak at 90.155 °C. In Dox-Gefit NPs and Dox-Gefit NPs-F, no endothermic peak was detected for Dox and Gefit, indicating that the drug was encapsulated in the biopolymeric core. Further, the endothermic peak obtained at 168.308 and 168.194 °C in the Dox-Gefit NPs and Dox-Gefit NPs-F corresponded to mannitol.

FT-IR Spectral Analysis. The FT-IR spectra of Dox, Gefit, cinnamon biopolymer, PVA, Dox-Gefit NPs, and Dox-Gefit NPs-F are displayed in Figure 8A−F. The IR absorption peak obtained at a wavenumber of 1620 cm^{-1} was due to C≡N stretching vibrations in Gefit, whereas absorption peaks at 1109 and 1011 cm^{-1} were related to C−O and C−F stretchings, respectively. A characteristic Dox absorption peak was at 1638 cm^{-1}. In the biopolymer, the absorption peak was around 2743.12 and 2918.33 cm^{-1}, belonging to the carboxylic acid group. The IR spectra of Dox-Gefit NPs and Dox-Gefit NPs-F showed that the majority of absorption bands were weaker in Gefit, demonstrating that the drug was entrapped in the NPs. On the other hand, the spectrum band at 1606 cm^{-1} in Dox-Gefit NPs-F was due to folate conjugation to the biopolymer surface.

Proton Nuclear Magnetic Resonance (^{1}H NMR). The formation of an amide bond (−$CONH_2$) between the primary amine group (−NH_2) of folic acid and the carboxylic acid group (−COOH) of Dox-Gefit NPs through conjugation is shown in

https://doi.org/10.1021/acsomega.3c01375
ACS Omega 2023, 8, 28165−28184

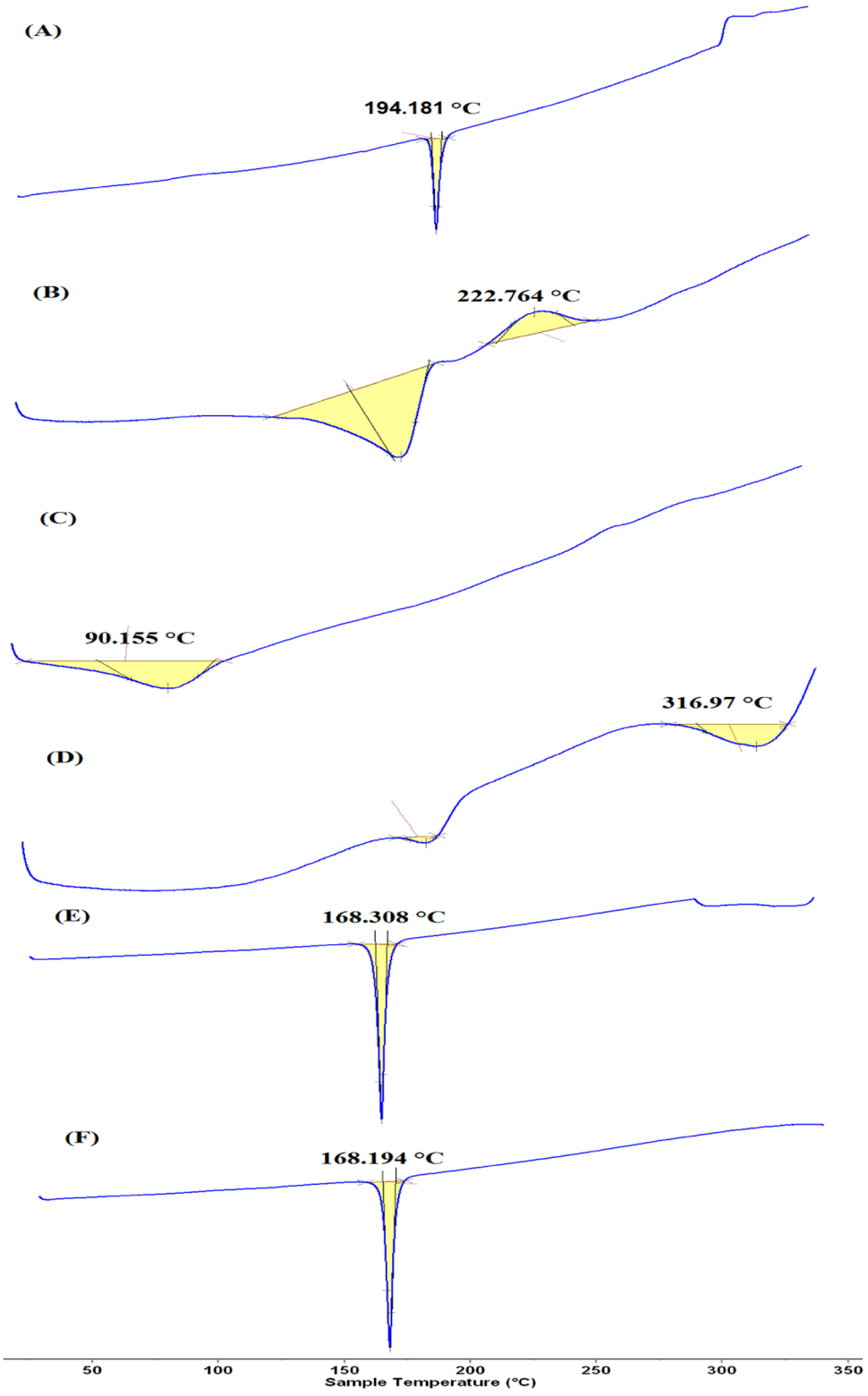

Figure 7. DSC thermogram Gefit (A), Dox (B), cinnamon biopolymer (C), PVA (D), Dox-Gefit NPs (E), and Dox-Gefit NPs-F (F).

Figure 9A. The ^{1}H NMR spectrum of amide linkage formation in Dox-Gefit NPs-F is shown in Figure 9B. The appearance of the ^{1}H NMR signals at 8.3088 ppm indicates the formation of amide bonds, which are formed via conjugation between the activated carboxylic acid group of the biopolymeric NPs and the primary amine group of folic acid.

X-ray Diffraction Analysis. Confirmation of the molecular state of Dox and Gefit in the NPs was further ensured through physicochemical characterization of the formulation using X-ray diffraction analysis. The X-ray diffraction patterns of Dox, Gefit, cinnamon biopolymer, Dox-Gefit NPs, and Dox-Gefit NPs-F are illustrated in Figure 10A–E. Sharp characteristic peaks are present for Gefit and Dox (Figure 10A,B), indicating their

https://doi.org/10.1021/acsomega.3c01375
ACS Omega 2023, 8, 28165−28184

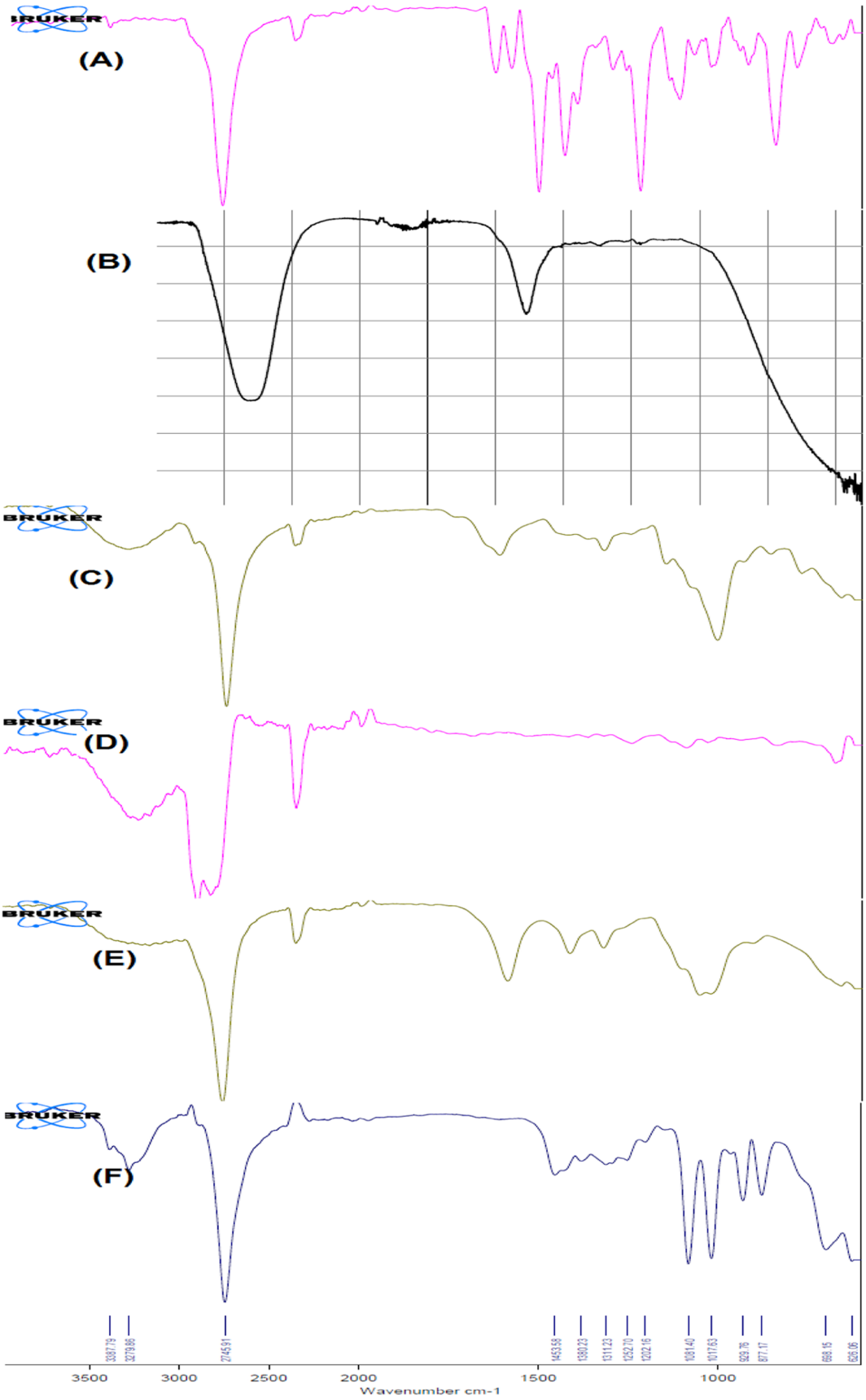

Figure 8. FT-IR spectra of Gefit (A), Dox (B), cinnamon polymer (C), PVA (D), Dox-Gefit NPs (E), and Dox-Gefit NPs−F (F).

crystalline nature. Peaks in the biopolymer (Figure 10C) appeared less crystalline due to some low-intensity peaks. However, the intensity of crystalline peaks was drastically reduced in the diffraction pattern of Dox-Gefit NPs and Dox-

https://doi.org/10.1021/acsomega.3c01375
ACS Omega 2023, 8, 28165−28184

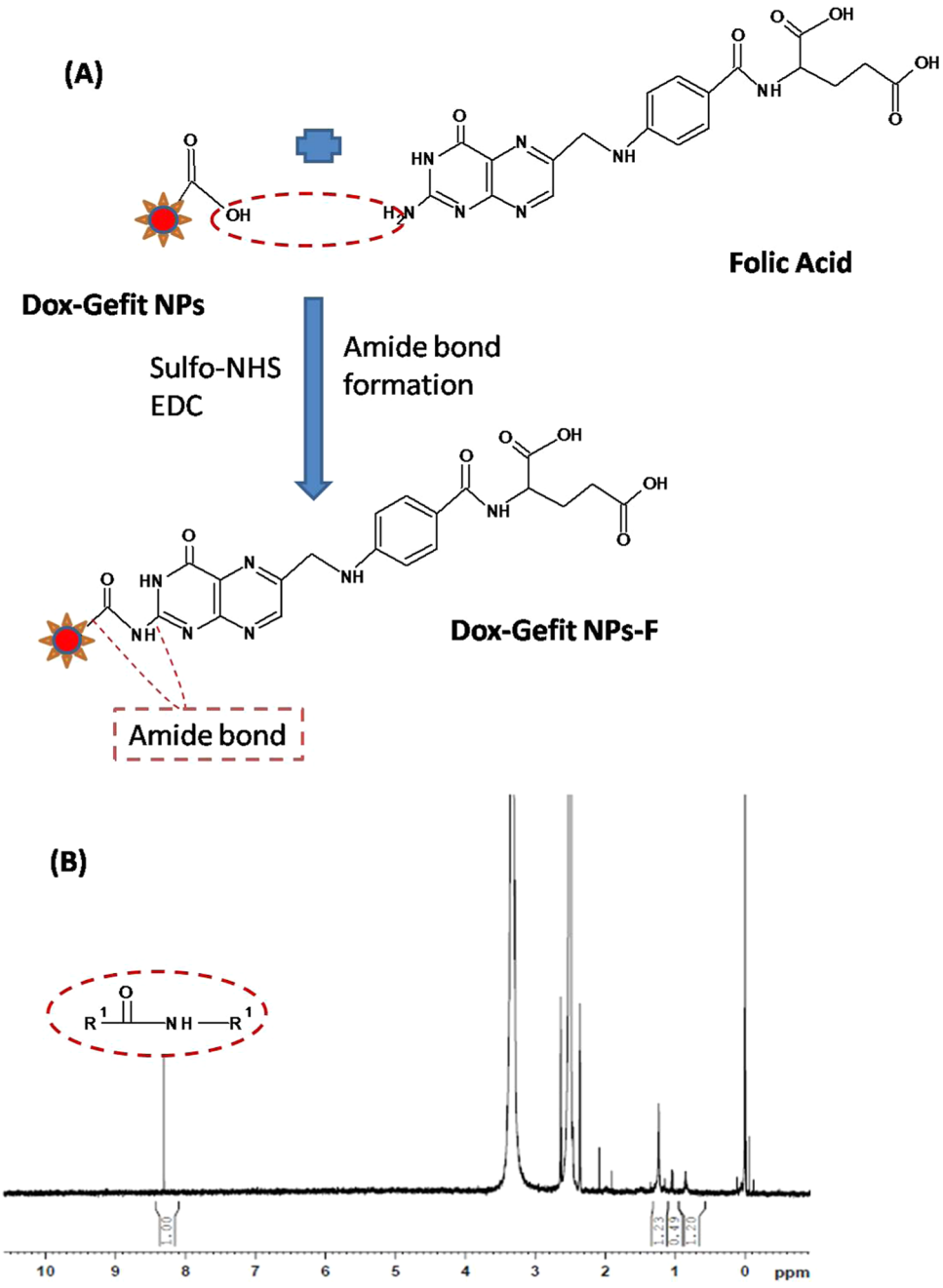

Figure 9. (A) Schematic diagram of amide-bond formation in Dox-Gefit NPs-F. (B) ^{1}H NMR spectrum of Dox-Gefit NPs-F.

Gefit NPs-F, revealing that Gefit and Dox were in an amorphous or molecular state in the biopolymeric core of the NPs, as shown in Figure 10D,E.

In Vitro Drug Release Studies. In vitro release studies were performed to investigate the release of Gefit and Dox from Dox-Gefit NPs and Dox-Gefit NPs-F in PBS of pH 7.4 and 5.4. The maximal amounts of Dox released at pH 7.4 were 60.87 ± 0.59 and 68.23 ± 0.125% from Dox-Gefit NPs and Dox-Gefit NPs-F, respectively. On the other hand, at pH 5.4, the maximum Dox released from Dox-Gefit NPs and Dox-Gefit NPs-F was 70.87 ± 0.28 and 80.23 ± 0.095%, respectively. Further, Gefit amounts released from Dox-Gefit NPs and Dox-Gefit NPs-F at pH 7.4 were 71.23 ± 0.1 and 80.21 ± 0.1%, respectively. Similarly, at pH 5.4, the maximum amounts of Gefit released were 69.24 ± 0.125 and 84.32 ± 0.58% as shown in Figure 11A,B.

KINETIC RELEASE MODELING

To understand the release mechanism of Dox and Gefit from Dox-Gefit NPs and Dox-Gefit NPs-F, the % drug release data at corresponding pH were fitted into multiple kinetic models. Based on best-fitting model correlation coefficients (R^2) at pH 7.4, the Korsmeyer−Peppas model was selected, with R^2 values of 0.9835 and 0.9926 for Dox release from Dox-Gefit NPs and Dox-Gefit NPs-F (Table 4). Further, the Korsmeyer−Peppas model was the best-fitting model for Gefit release from both formulations, with R^2 values of 0.9809 and 0.9800 at pH 7.4, respectively.

On the other hand, at pH 5.4, among the various models, the Korsmeyer−Peppas model was selected as the best-fitting model, with an R2 value of 0.9834 for Dox release from Dox-Gefit NPs. The first order for release of Dox from Dox-Gefit

https://doi.org/10.1021/acsomega.3c01375
ACS Omega 2023, 8, 28165−28184

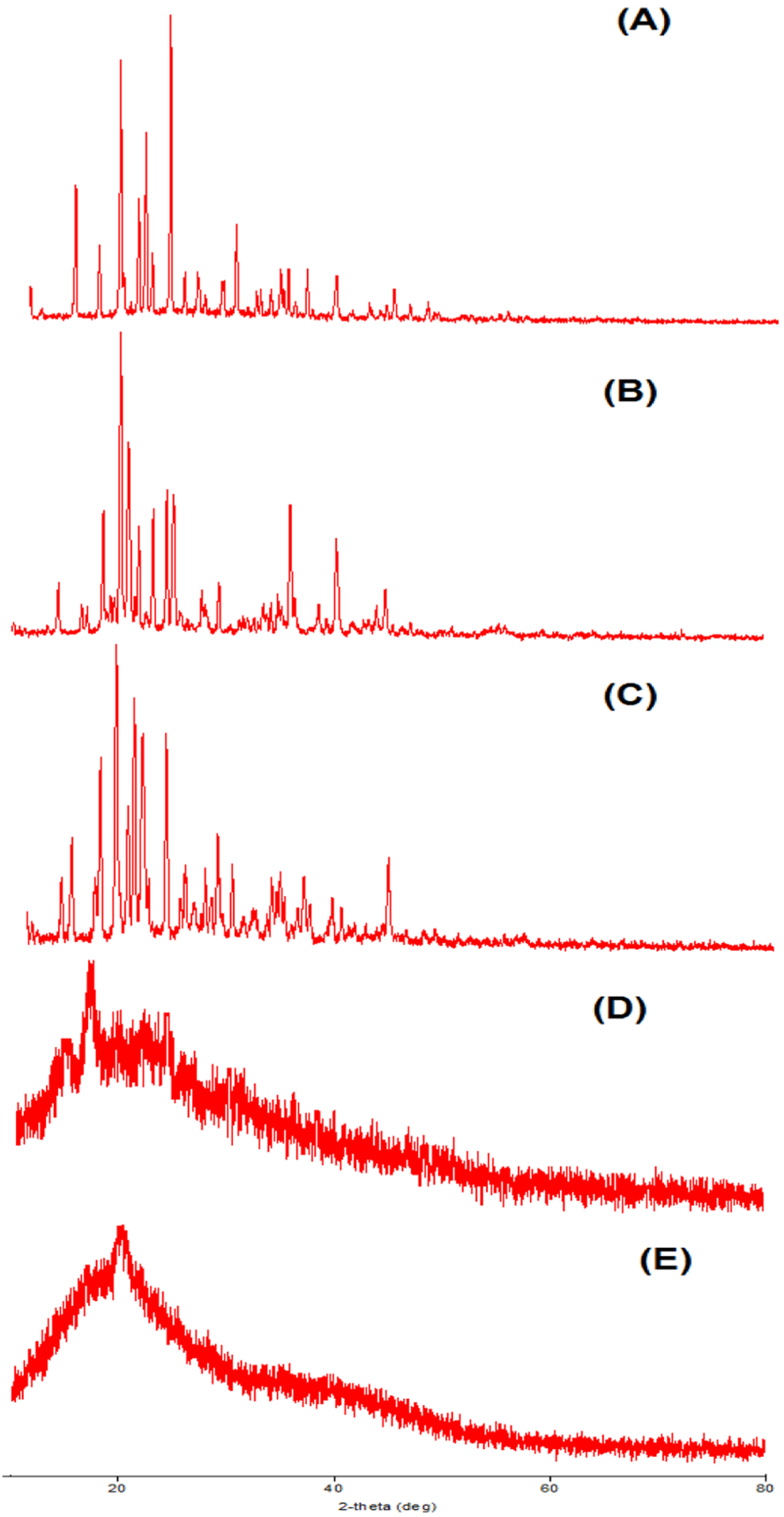

Figure 10. XRD diffraction analyses of (A) Gefit, (B) Dox, (C) cinnamon biopolymer, (D) Dox-Gefit NPs, and (E) Dox-Gefit NPs-F.

NPs-F had an R2 value of 0.9893. Gefit release from Dox-Gefit NPs and Dox-Gefit NPs-F at pH 5.4 showed the Korsmeyer–Peppas model of good fit with R2 values 0.9665 and 0.9737 (Table 5). These kinetic release modeling outcomes suggest that

https://doi.org/10.1021/acsomega.3c01375
ACS Omega 2023, 8, 28165−28184

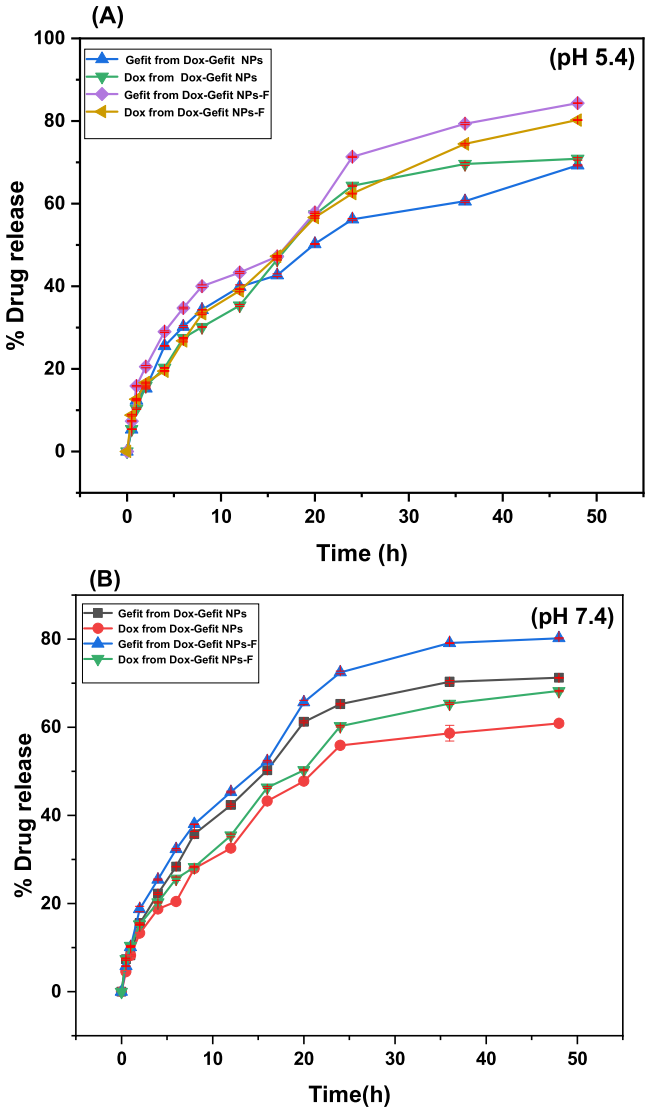

Figure 11. In vitro drug release of Gefit and Dox. (A) pH 5.4 and (B) pH 7.4.

simultaneous release of Dox and Gefit was caused by swelling and hydration of the polymeric matrix, and thereby water diffusion into polymeric NPs results in the improved release.[48]

HEMOLYSIS STUDIES

A hemolysis assay was performed to ensure that the developed formulation would be safe in the bloodstream. A nanomaterial used for therapeutic purposes in the systemic circulation must be biocompatible and unharmful to blood cells. Nano-biointeractions may damage erythrocytes and liberate hemoglobin. Hemocompatibility in accordance with the Standard Practice for Assessment of Hemolytic Properties of Materials from the American Society for testing and Materials (ASTM756, 2000) suggested 5% destruction of blood cells categorized as hemolytic.

Increasing the doses of NPs led to increased hemoglobin release from erythrocytes (Figure 12A,B). Hemolytic analysis revealed that RBC damage was <6−8% at 1.5, 3, or 6 mg, corresponding to placebo NPs, Dox-Gefit NPs, and Dox-Gefit NPs-F. The nNormal saline was safe to blood, and the highest RBS destruction was seen with triton-X-100.

CELL VIABILITY ASSAY AND DETERMINATION OF THE COMBINATION INDEX (CI)

The cytotoxic activity of the formulations was found to be concentration- and time-dependent (Figure 13A,B). The Dox-Gefit NPs-F significantly depleted the viable cell count to 30.33 ± 0.5% as compared to Dox-Gefit-NPs at 64.33 ± 0.5% and pure Dox and pure Gefit at 86.5 ± 3.98 and 91.5 ± 4.74% in glioma C6 cells after 24 h of incubation. In contrast, Dox-Gefit NPs-F reduced the viable cell count to 26 ± 3.6% compared to Dox-Gefit NPs at 66.33 ± 2.31% and pure Dox and pure Gefit at 85.2 ± 1.89 and 92.0 ± 5.84% in glioma U87 cells. The cell viability of the selected cancer cell lines decreased in response to the increasing pharmaceutical dose loaded in the NPs.

IC50 values for pure Dox-Gefit, Dox-Gefit NPs, and Dox-Gefit NPs-F were 25.88, 9.9, and 3.19 μM, respectively, in the U87 cell line. In the C6 glioma cell line, the IC50 values of pure Dox-Gefit, Dox-Gefit NPs, and Dox-Gefit NPs-F were 26.64, 8.43, and 3.31 μM, respectively. The CI values determined for codelivery of Dox-Gefit from Dox-Gefit NPs-F in U87 and C6 cell lines were 0.201 and 0.199, respectively. MTT assay outcomes showed that Dox-Gefit NPs-F decreased the cell viability based on receptor-mediated cellular entry into cancer cells. The addition of folate decoration to the NP surface facilitates membrane receptor binding and enables selective internalization, leading to enriching the drug concentration in the cancer cells.[39]

Biodistribution Studies. Tissue homogenates from the heart, liver, kidney, brain, lungs, and blood were extracted in an organic solvent and analyzed by HPLC for the presence of Dox and Gefit. A significant amount of Dox and Gefit was measured in the brain compared to the drug suspension ($p < 0.05$). The biodistribution studies of the formulations in various organs are shown in Figure 14.

Stability Studies. A stability study was performed as per guidelines issued under the stability testing of pharmaceuticals [ICH Q1A (R2)]. The Dox-Gefit NPs and Dox-Gefit NPs-F stability experiments are summarized in Tables 6 and 7. Dox-Gefit NPs and Dox-Gefit NPs-F particle sizes were measured to be 122.52 ± 4.46 nm and 124.45 ± 6.37 at 25 ± 2 °C, 65 ± 5%

Table 4. Kinetic Release of Dox and Gefit from Dox-Gefit NPs and Dox-Gefit NPs-F at pH 7.4

	Dox release from Dox-Gefit NPs at pH 7.4		Dox release from Dox-Gefit NPs-F at pH 7.4		Gefit release form Dox-Gefit NPs at pH 7.4		Gefit release form Dox-Gefit NPs-F at pH 7.4	
model fitting	R^2	k	R^2	k	R^2	k	R^2	k
zero order	0.8460	1.3153	0.8718	1.4358	0.8218	1.5390	0.8419	1.7228
first order	0.9042	−0.0211	0.9395	−0.0251	0.9026	−0.0285	0.9384	−0.0368
Higuchi Matrix	0.9266	8.6267	0.9195	9.1017	0.9290	9.4093	0.9263	9.8482
Korsmeyer−Peppas	0.9835	2.4618	0.9926	2.7676	0.9809	2.7420	0.9800	2.7868
Hixon− Crowell	0.8868	0.0060	0.9203	0.0069	0.8788	0.0076	0.9129	0.0093

https://doi.org/10.1021/acsomega.3c01375
ACS Omega 2023, 8, 28165−28184

Table 5. Kinetic Release of Dox, Gefit from Dox-Gefit NPs, and Dox-Gefit NPs-F at pH 5.4

	Dox release from Dox-Gefit NPs at pH 5.4		Dox release from Dox-Gefit NPs-F at pH 5.4		Gefit release form Dox-Gefit NPs at pH 5.4		Gefit release form Dox-Gefit NPs-F at pH 5.4	
model fitting	R^2	k	R^2	k	R^2	k	R^2	k
zero order	0.8582	1.5360	0.9124	1.6531	0.8461	1.3428	0.8782	1.6858
first order	0.9248	−0.0280	0.9893	−0.0338	0.9418	−0.0234	0.9736	−0.0384
Higuchi Matrix	0.9233	9.3320	0.9161	9.7072	0.9211	8.7608	0.9128	9.8343
Korsmeyer−Peppas	0.9834	2.6574	0.9884	2.9137	0.9665	2.7818	0.9737	3.0861
Hixon−Crowell	0.9062	0.0076	0.9721	0.0087	0.9143	0.0064	0.9534	0.0095

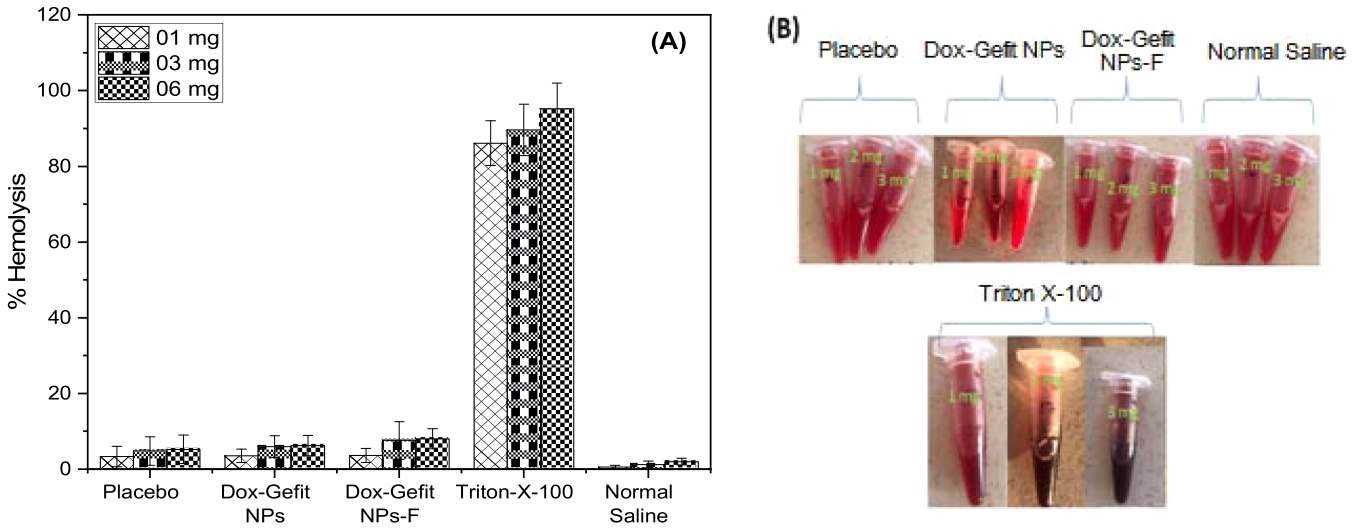

Figure 12. Hemolysis of NPs. (A) Percentage hemolysis with placebo NPs, Dox-Gefit NPs, Dox-Gefit NPs-F, Triton-X-100, and normal saline. (B) Tubes containing blood after exposure to NPs, normal saline, or Triton-X-100.

RH at the end of 90 days. At an elevated temperature of 40 ± 2 °C, 75 ± 5% RH, sizes were 123.23 ± 24.68 and 126.45 ± 5.76 nm with the same duration of storage. Similarly, surface charges on the Dox-Gefit NPs and Dox-Gefit NPs-F at temperatures of 25 ± 2 °C, 65 ± 5% RH and 40 ± 2 °C, 75 ± 5% RH were −20.3 ± 3.11, −22.4 ± 5.41 and −21.5 ± 2.23, −23.6 ± 2.55 mV, respectively, after 90 days. The % entrapment efficiencies of Dox from Dox-Gefit NPs and Dox-Gefit NPs-F were 75 ± 7.3 and 76 ± 8.2% at 25 ± 2 °C, 65 ± 5% RH; and 74 ± 9.3 and 75 ± 6.2% at 40 ± 2 °C, 75 ± 5% RH, respectively, after 90 days. Moreover, the entrapment efficiencies of Gefit from Dox-Gefit NPs and Dox-Gefit NPs-F were 73 ± 6.6 and 76 ± 8.2% at 25 ± 2 °C or 65 ± 5% RH; and 72 ± 9.6 and 74 ± 6.2% at 40 ± 2 °C, 75 ± 5% RH after a period of 90 days.

FBS STABILITY OF DOX-GEFIT-NPS-F

The stability of Dox-Gefit NPs-F in 10% FBS is shown in Figure 15. UV scanning of NPs after incubation for 1 h revealed a decrease in absorbance at the wavelength of 298 nm, as indicated by the red line bar. Moreover, after 6 h, a higher absorbance was recorded, exhibiting the layering of protein molecules onto the NP surface. The variation in physicochemical properties such as particle size of Dox-Gefit NPs-F in 10% FBS indicated that it was increased after 1 h of incubation, and thereafter, a drop in particle size was noticed until 24 h.

DISCUSSION

Intranasal drug delivery is a noninvasive alternative to intravenous or intramuscular delivery. This route allows easy access of active substances to the CNS, bypassing the blood−brain barrier and first-pass metabolism. It offers a large surface area of nasal septum that connects directly to the brain. The porous nasal mucosa membrane has high blood flow and allows high drug diffusion, partitioning, and access.[49] The NP drug delivery system is quickly taken up into the blood and reaches out to the brain via the nasal route. NPs carrying therapeutics in biopolymers, with their surface tuned with the ligand, are more specifically taken up by cancer cell surface receptors, providing prolonged drug release, which could be effective in glioma therapy due to better cellular internalization of therapeutics.[50,51] For decades, NPs have had potential as drug delivery vectors for a vast number of biological and therapeutic substances. The BBB and blood−brain tumor barrier (BBTB) are potential roadblocks for the transport of molecules, resulting in subtherapeutic drug effects in the CNS. Nanotechnology may improve the capability of nanocarriers to avoid this block when treating various brain disorders including gliomas. Nanotechnology may help optimize particle size and sizing to around 100 nm or less and may preferentially transport across the blood−brain barrier to deliver the drugs to the target site.[52] The present study developed, characterized, and evaluated Dox-Gefit NPs and folate-armored Dox-Gefit NPs-F for targeting glioma via the nose-to-brain route.

The formulations were nanosized, with particle diameters of 109.45 ± 7.26 and 120.35 ± 3.65 nm for NPs and surface-functionalized NPs. They exhibited a sustained release behavior for both Dox and Gefit at physiological pH 7.4 and endosomal pH 5.4.[37] The PDI values of Dox-Gefit NPs and Dox-Gefit NPs-F were 0.107 and 0.110, indicating the preparations were homogeneous, monodisperse, and consistent and had narrow particle size distributions.[53,54] TEM analysis revealed that the

https://doi.org/10.1021/acsomega.3c01375
ACS Omega 2023, 8, 28165−28184

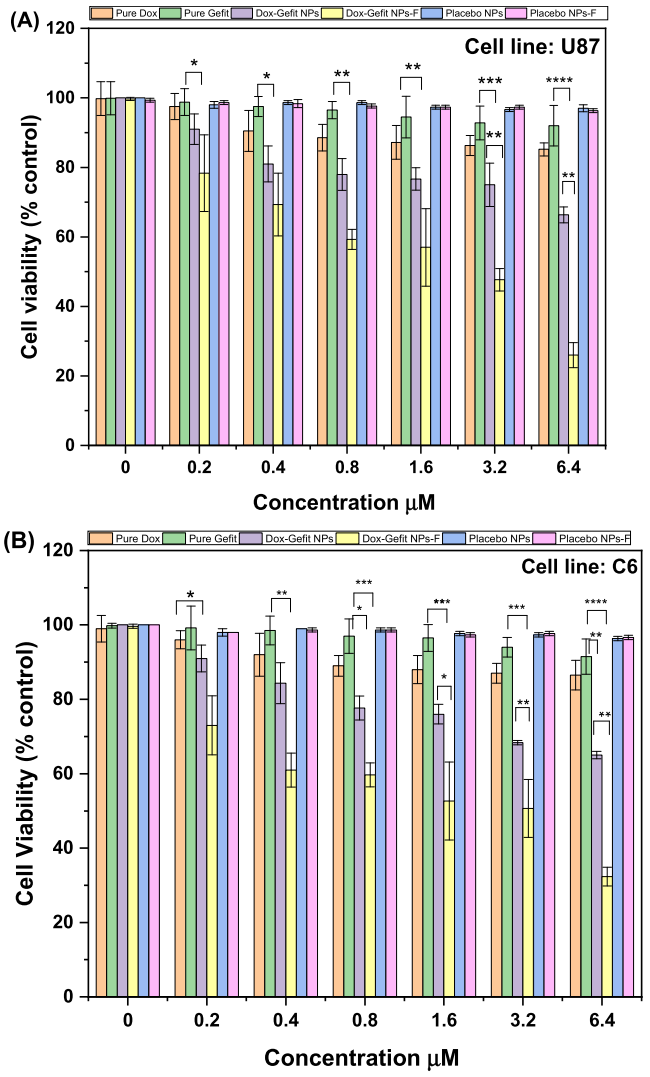

Figure 13. Cell viability study. (A) Bar graph showing the percentage U87 cell viability after 24 h treatment with different concentrations of pure Dox, pure Gefit, Dox-Gefit NPs, Dox-Gefit NPs-F, placebo NPs, or placebo NPs-F, and (B) showing cell viability in the C6 glioma cell line after 24 h of the same treatment. The bar graphs show the mean ± S.D. ($n = 3$). Level of significance *($p < 0.05$), **($p < 0.01$), ***($p < 0.001$), ****($p < 0.0001$) compared to pure Dox and pure Gefit.

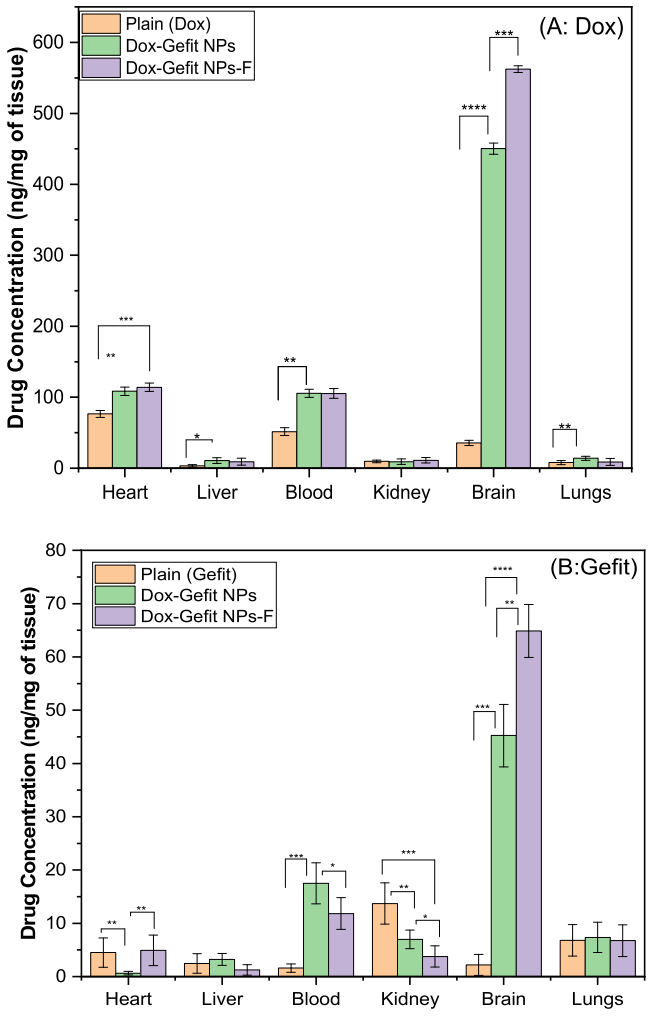

Figure 14. Biodistribution of Dox and Gefit in the heart, liver, kidney, brain, blood, and lungs. (A) Dox concentration from plain Dox, Dox-Gefit NPs, and Dox-Gefit NPs-F; (B) Gefit concentration from plain Gefit, Dox-Gefit NPs, and Dox-Gefit NPs-F.

NP formulations were well-dispersed, separated, uniform, and consistent in size, in agreement with results from the Malvern zetasizer. The ζ potential value indicated a negative surface charge on NPs, illustrating nonagglomeration of the NPs, probably due to their tendency to repel similar charges on neighboring molecules, overall leading to improved stability of the nanosized system.[55]

Free Dox and Gefit may show toxicity to the vital organs of the body, especially in the brain, heart, liver, lungs, and kidneys. However, biopolymer encapsulation may reduce these toxic side effects after systemic administration. The biobased polymer used in the current study was obtained from *C. Zeylanicum* and employed as a drug carrier to deliver drug to the target tumor site with reduced or no toxicity. The cytotoxicity studies showed no toxicity of biopolymer, demonstrating its safe and biocompatible nature.[56,57]

The FT-IR spectra of Dox-Gefit NPs and Dox-Gefit NPs-F showed that the characteristic Gefit absorption band was weaker, demonstrating that it was entrapped in the NPs and compatible with the other excipients used in the formulation.[58] In the FT-IR spectrum of Dox-Gefit NPs-F, the absorption peak appeared at 1606 cm^{-1} and revealed successful ligation of folic acid with Dox-Gefit NPs. The DSC study of Dox-Gefit NPs and Dox-Gefit NPs-F showed no endothermic peaks, indicating that it might be encapsulated in the biopolymeric core and remain in the dissolved state in the NP. The molecular state of both drugs in the polymeric matrix was confirmed by an XRD study, with minimal or no formation of polymorphs.[59]

Surface functionalization of NPs with folic acid was confirmed by ^{1}H NMR analysis and can be compared to folate ligation with 5-fluorouracil-loaded chitosan NPs from Ullah and associates.[60] In ^{1}H NMR, the appearance of signals at 8.3088 ppm indicated amide-bond formation through a reaction between the activated ester group of polymeric NPs and the primary amino group of the folic acid. Therefore, Dox-Gefit NPs-F was synthesized as indicated by the formation of an amide bond.[61]

Initially, both Dox and Gefit releases from the biopolymer were abrupt but then became controlled and sustained over a long time. The abrupt release from the biopolymer may be due to some drugs being embedded or adsorbed on the polymeric surface or to the exterior layer of the biopolymer. However, the

https://doi.org/10.1021/acsomega.3c01375
ACS Omega 2023, 8, 28165−28184

Table 6. Stability of Dox-Gefit NPs, Related to Particle Size, ζ Potential, and % Entrapment Efficiency

sampling period (in days)	particle size (nm)		% ζ potential (mV)		entrapment efficiency (Dox)		entrapment efficiency (Gefit)	
	(25 ± 2 °C, 65 ± 5% RH)	(40 ± 2 °C, 75 ± 5% RH)	(25 ± 2 °C, 65 ± 5% RH)	(40 ± 2 °C, 75 ± 5% RH)	(25 ± 2 °C, 65 ± 5% RH) (%)	(40 ± 2 °C, 75 ± 5% RH) (%)	(25 ± 2 °C, 65 ± 5% RH) (%)	(40 ± 2 °C, 75 ± 5% RH) (%)
0	109.45 ± 7.26	109.45 ± 7.26	−18.0 ± 3.27	−8.0 ± 3.27	82 ± 4.2	82 ± 4.2	77 ± 5.6	77 ± 5.6
30	109.99 ± 8.34	110.62 ± 9.32	−18.7 ± 7.40	−19.6 ± 4.21	79 ± 6.3	78 ± 5.3	76 ± 3.9	76 ± 8.9
60	115.32 ± 3.33	112.25 ± 16.35	−19.8 ± 3.00	−21.5 ± 3.35	77 ± 8.9	76 ± 5.4	74 ± 6.7	74 ± 3.7
90	122.52 ± 4.46	123.23 ± 24.68	−20.3 ± 3.11	−21.5 ± 2.23	75 ± 7.3	74 ± 9.3	73 ± 6.6	72 ± 9.6

Table 7. Stability of Dox-Gefit NPs-Fs, Related to Particle Size, ζ Potential, and % Entrapment Efficiency

sampling period (in days)	particle size (nm)		% ζ potential (mV)		entrapment efficiency (Dox)		entrapment efficiency (Gefit)	
	(25 ± 2 °C, 65 ± 5% RH)	(40 ± 2 °C, 75 ± 5% RH)	(25 ± 2 °C, 65 ± 5% RH)	(40 ± 2 °C, 75 ± 5% RH)	(25 ± 2 °C, 65 ± 5% RH) (%)	(40 ± 2 °C, 75 ± 5% RH) (%)	(25 ± 2 °C, 65 ± 5% RH) (%)	(40 ± 2 °C, 75 ± 5% RH) (%)
0	120.35 ± 3.65	120.35 ± 3.65	−20.0 ± 8.23	−20.0 ± 8.23	83 ± 2.9	83 ± 2.9	78 ± 6.67	78 ± 6.67
30	121.34 ± 5.24	122.34 ± 5.23	−21.5 ± 6.35	−22.9 ± 8.33	80 ± 3.9	79 ± 3.3	77 ± 5.2	77 ± 7.2
60	122.43 ± 4.42	124.35 ± 6.36	−21.5 ± 5.30	−23.4 ± 5.66	79 ± 3.9	78 ± 7.3	76 ± 7.5	75 ± 4.2
90	124.45 ± 6.37	126.56 ± 5.76	−22.4 ± 5.41	−23.6 ± 2.55	76 ± 8.2	75 ± 6.2	75 ± 6.2	74 ± 6.2

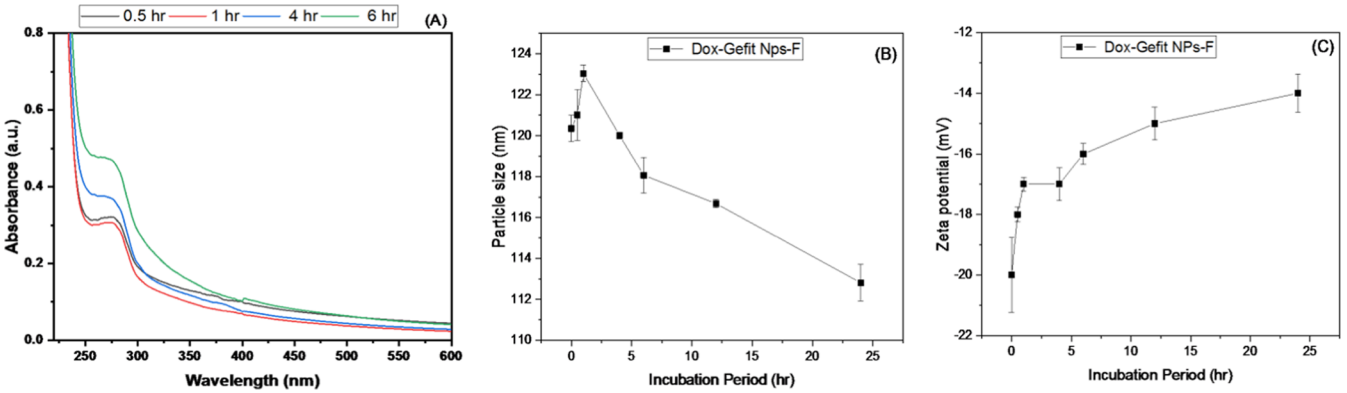

Figure 15. Nanodrug stability in 10% FBS. UV spectrum of Dox-Gefit NPs-F incubated in 10% FBS at corresponding times of 0.5, 1, 4, and 6 h (A); alternation in particle size (B) and ζ potential of Dox-Gefit NPs-F (C) at the end of 24 h.

major part of the drugs are encapsulated in the interior layer of the biopolymeric carrier, exhibiting a sustained release profile over a period of 48 h. We further observed that Gefit and Dox release was elevated at acidic intracellular endosomal pH 5.4 from Dox-Gefit NPs-F as compared to that at pH 7.4.[62,63] It is notable that the tumor microenvironment is more acidic than physiological fluid. The higher level of drug release at acidic pH may be attributed to protonation (H^+) of the carboxyl group in the biopolymer from (NH_3^+) of Dox (pK_a = 8.2) and Gefit (pK_a = 5.4−7.2), resulting in higher dissociation or dissolution of Dox and Gefit from the polymeric complex of NPs in the acidic environment.[64] The low drug release at physiological pH may be ascribed to the poor protonation on the carboxyl group in the biopolymer ensuing higher drug/polymer interaction. It is worthy to minimize drug release from the carrier at physiological pH in systemic circulation until the target is achieved. Further, it was noted that folate conjugated, Dox-Gefit NPs-F showed a higher release than Dox-Gefit NPs probably due to the longer retention at pH 5.4. The acidic pH microenviroment of cancer cells is favorable for drug release from polymeric carriers while also minimizing release in nontarget areas, including the systemic circulation. The functionalized nanodrug carrier system provides appropriate drug concentrations in the target after successful cell uptake, and internalization is mediated via endosomal escape and lysosomal fusion in the cytoplasm.[65] The kinetic release results suggested that the simultaneous release of Dox and Gefit was caused by swelling of the polymeric matrix, dissolution, and water migration into polymeric NPs.[66]

The hemolysis assay showed that the concentration of formulation tested for hemocompatibility was safe and compatible with the biological system. The study outcomes unveiled here are in agreement with a previous work.[67] The developed formulations were conceived to be nontoxic and regarded as safe and compatible with blood for in vivo administration. Further hemolysis assays suggested that biopolymers may be nontoxic and their use might minimize the potential hazards of cytotoxicity caused by synthetic drug carriers or unmodified carriers.[68−70]

The IC50 values of the NPs were measured in the glioma cancer cell lines U87 and C6.[71] The cell-killing potency of the formulations was dose- and time-dependent. The cell viability decreased in response to the dose of pharmaceuticals loaded in NPs and functionalized NPs. The MTT assay outcomes suggested that Dox-Gefit NPs-F successfully decreased cell viability with increasing concentration of the drug in the NPs owing to improved drug delivery into the cells.[71,72] Further, the combination index value was investigated, which indicated the synergistic effect of both drugs from Dox-Gefit NPs-F, and it was verified using the Chou−Talalay method.[73,74] It has been reported that tumor cells overexpressing the folate receptor

https://doi.org/10.1021/acsomega.3c01375
ACS Omega 2023, 8, 28165−28184

could be an easy route of access for cytotoxic drugs.[55,71] In the current study, folate ligation to Dox-Gefit NPs resulted in a higher brain concentration compared to bare NPs, validating the higher efficacy of Dox-Gefit NPs-F. There was also remarkable cytotoxicity of Dox-Gefit NPs-F compared to bare NPs, comparable to a previous study executed by Jingjing et al. and Mondal and associates.[35,75]

Biodistribution studies were conducted as per the literature by the intranasal route, followed by estimation of the drug plasma concentration using HPLC.[48] Therapeutic concentrations of drug were achieved in the brain via overcoming the permeation barrier. Folate functionalized NPs had the potential to cross the barrier and reach targets in the brain. In addition, drug concentrations were also achieved in nontargeted organs like the blood, heart, liver, lungs, and kidney due to diffusion and the partitioning behavior of the nanosized Dox-Gefit NPs and Dox-Gefit NPs-F. However, the concentrations of Dox and Gefit in the target brain tissue were significantly higher than in the other organs of the body.[72] Farheen and associates in a preceding work designed, characterized, and evaluated folate anchored Dox-Erlo containing biopolymeric nanoparticles (Dox-Erlo NP conjugates) against glioma cancer. It was found that the percentage releases of Dox and Gefit from Dox-Gefit NPs-F were significantly higher in PBS pH 7.4 and pH 5.4 than the Dox and Erlo release from Dox-Erlo-NP conjugates ($p < 0.05$). Moreover, the authors observed a noticeable variation in the biodistribution of Dox in the brain from Dox-Gefit NPs-F compared to the Dox-Erlo NP conjugates. It was noted a significant improvement in the biodistribution of Dox in the brain, i.e., 0.562 μg/mg of the brain tissue from Dox-Gefit NPs-F compared to 40 ng/g of the brain tissue from Dox-Erlo NPs conjugates, indicating the superior therapeutic efficacy of the Dox-Gefit NPs-F over Dox-Erlo NP conjugates ($p < 0.01$).[75]

As per the experimental observation, the stability of Dox-Gefit NPs and Dox-Gefit NPs-F was maintained because the changes in the particle size, ζ potential, and entrapment efficiency were insignificant after analysis of the sample at a fixed interval of time in a storage period of 90 days ($p > 0.05$). This further indicates that the in-house-developed Dox-Gefit NPs and Dox-Gefit-F were robust, stable, and consistent, and thus, impacts on the physicochemical stability of NPs under the storage condition for a designated period of 90 days remain unaffected.[44,45] Incubating Dox-Gefit NPs-F in FBS led to interaction with the NP surface, making an area of nano-biointeraction probably due to NP charge surfaces, and this interaction was witnessed for a short time. Thereafter, reduction in the particle size was observed may be due to the drug release over time. Moreover, the increase and decrease in particle size after incubation of 24 h were not significantly different ($p > 0.05$), demonstrating the nanodrug stability in the biological medium. Similarly, the ζ potential of Dox-Gefit NPs-F was also measured over the time of the study, indicating a change in the surface charge. This change may be due to the positive interaction of macromolecules with the NP surface. The change in the ζ potential was measured in between −20 and −14 mV. The study report discussed herein was accompanied by a previous work by Palanikumar et al. in polymeric nanoparticles for targeted drug delivery in cancer.[76]

CONCLUSIONS

Here, we successfully designed biobased polymer NPs encapsulating Dox-Gefit by a double-emulsion solvent evaporation method. The surface of the NPs was functionalized with folic acid for receptor-based targeting in glioma. Proton (^{1}H) NMR studies revealed successful conjugation of the folate to the biopolymeric surface. The optimized functionalized formulation comprised the biopolymer at 2.19%w/v and surfactant PVA at 1.73%w/v and used a sonication time of 8.6 min for a stable and robust preparation. The measured particle size of the functionalized biopolymeric NPs was 109.45 nm, with a PDI of 0.107 and a ζ potential of −20.0 ± 8.23 mV. This enabled crossing of the blood−brain barrier to reach therapeutic drug concentrations. The Korsmeyer−Peppas model was the best-fitted kinetic model for drug release from the nanocarrier. It was based on swelling and hydration of the biopolymeric matrix and consequently improved release. DSC analysis showed Dox and Gefit were encapsulated within the biopolymeric core. FT-IR analysis demonstrated that the minor shift in the spectrum in Dox-Gefit NPs-F was due to folate conjugation to the biopolymer. The Dox-Gefit NPs-F inhibited cell growth in C6 and U87 glioma cell lines due to the enhanced transport of Dox and Gefit, resulting in improved cytotoxicity. A hemolysis assay showed that Dox-Gefit NPs-F are safer to systemic circulation. Biodistribution measured a significant amount of Dox and Gefit in the brain. The cytotoxicity studies demonstrated that the developed Dox-Gefit NPs-F could be efficacious against U87 and C6 cell lines. Based on these findings, Dox-Gefit NPs-F could potentially be effective in glioma cancer treatment and may be translated into clinic.

AUTHOR INFORMATION

Corresponding Author

Md Habban Akhter − *School of Pharmaceutical and Population Health Informatics (SoPPHI), DIT University, Dehradun, Uttrakhand 248009, India;* orcid.org/0000-0001-6278-0370; Email: habban.akhter@dituniversity.edu.in, habban2007@gmail.com

Authors

Ms Farheen − *School of Pharmaceutical and Population Health Informatics (SoPPHI), DIT University, Dehradun, Uttrakhand 248009, India*

Havagiray Chitme − *School of Pharmaceutical and Population Health Informatics (SoPPHI), DIT University, Dehradun, Uttrakhand 248009, India*

Muath Suliman − *Department of Clinical Laboratory Sciences, College of Applied Medical Sciences, King Khalid University, Abha 62521, Saudi Arabia*

Mariusz Jaremko − *Smart-Health Initiative (SHI) and Red Sea Research Center (RSRC), Division of Biological and Environmental Sciences and Engineering (BESE), King Abdullah University of Science and Technology (KAUST), Thuwal 23955-6900, Saudi Arabia*

Abdul-Hamid Emwas − *Core Labs, King Abdullah University of Science and Technology (KAUST), Thuwal 23955-6900, Saudi Arabia*

Complete contact information is available at: https://pubs.acs.org/10.1021/acsomega.3c01375

Author Contributions

Conceptualization, M.H.A. and M.F.; methodology, M.H.A. and M.F.; software, M.H.A. and M.F.; validation, M.H.A. and M.F.; formal analysis, M.H.A., M.F., and H.C.; investigation, M.H.A. and H.C.; resources, M.J. and A-H.E.; data curation, M.F. and M.H.A.; writing—original draft preparation, M.F.; writing—review and editing, M.H.A., H.C., and A.-H.E.; visualization, M.S., M.J., and A.-H.E.; supervision, M.H.A. and C.H.; project

https://doi.org/10.1021/acsomega.3c01375
ACS Omega 2023, 8, 28165−28184

administration, M.H.A. and C.H.; funding acquisition, M.S., M.J., and A.-H.E. All authors have read and agreed to the published version of the manuscript.

Notes

The authors declare no competing financial interest.

This work has been patented as Indian Patent Application No. 202111053842. Publication Date, 03/12/2021.

■ ACKNOWLEDGMENTS

The authors are thankful to the DIT University, School of Pharmaceutical and Population Health Informatics (SoPPHI), Dehradun, India, for providing the facility to conduct the work. They extend their appreciation to the Deanship of Scientific Research at King Khalid University for supporting this work through a general research program under grant number RGP.02/214/43. M.J. and Abdel thank the King Abdullah University of Science and Technology, Saudi Arabia, for support.

■ REFERENCES

(1) Lin, Y. K.; Wang, S. W.; Lee, R. S. Redox-responsive dasatinib-containing hyaluronic acid prodrug and co-delivery of doxorubicin for cancer therapy. *Int. J. Polym. Mat. Poly. Biomat.* **2021**, *70*, 1329−1343.

(2) Henriksen, O. M.; Del, M. Á. M.; Figueiredo, P.; Hangel, G.; Keil, V. C.; Nechifor, R. E.; Riemer, F.; Schmainda, K. M.; Warnert, E. A. H.; Wiegers, E. C.; Booth, T. C. High-Grade Glioma Treatment Response Monitoring Biomarkers: A Position Statement on the Evidence Supporting the Use of Advanced MRI Techniques in the Clinic, and the Latest Bench-to-Bedside Developments. Part 1: Perfusion and Diffusion Techniques. *Front. Oncol.* **2022**, *12*, No. 810263.

(3) Baskin, D. S.; Sharpe, M. A.; Nguyen, L.; Helekar, S. A. Case Report: End-Stage Recurrent Glioblastoma Treated With a New Noninvasive Non-Contact Oncomagnetic Device. *Front. Oncol.* **2021**, *11*, No. 708017.

(4) Stephen, J. B.; Shawn, K.; Rifaquat, R.; Eudocia, Q.; Lee, G. P.; Dunn, E. G.; Susan, M.; Chang, L. B. N.; Manmeet, S.; Ahluwalia, R. S.; Minesh, P.; Mehta, D. A. Glioblastoma Clinical Trials: Current Landscape and Opportunities for Improvement. *Clin. Cancer Res.* **2022**, *15*, 594−602.

(5) Dong, X. Current Strategies for Brain Drug Delivery. *Theranostics* **2018**, *8*, 1481−1493.

(6) Norouzi, M.; Yathindranath, V.; Thliveris, J. A.; et al. Doxorubicin-loaded iron oxide nanoparticles for glioblastoma therapy: a combinational approach for enhanced delivery of nanoparticles. *Sci. Rep.* **2020**, *10*, 11292.

(7) Finch, A.; Solomou, G.; Wykes, V.; Pohl, U.; Bardella, C.; Watts, C. Advances in Research of Adult Gliomas. *Int. J. Mol. Sci.* **2021**, *22*, 924.

(8) Shoufeng, W.; Junde, L. Efficacy and Safety of Temozolomide Combined with Radiotherapy in the Treatment of Malignant Glioma. *J. Healthcare Eng.* **2022**, *6*, No. 3477918.

(9) Yudintceva, N.; Lomert, E.; Mikhailova, N.; Tolkunova, E.; Agadzhanian, N.; Samochernych, K.; Multhoff, G.; Timin, G.; Ryzhov, V.; Deriglazov, V.; et al. Targeting Brain Tumors with Mesenchymal Stem Cells in the Experimental Model of the Orthotopic Glioblastoma in Rats. *Biomedicines* **2021**, *1*, No. 1592.

(10) Xu, H-L.; Mao, K-L.; Huang, Y-P.; Yang, J-J.; Xu, J.; Chen, P-P.; Fan, Z-L.; Zou, S.; Gao, Z-Z.; Yin, J-Y.; Xiao, J.; Lu, C-T.; Zhang, B-L.; Zhao, Y-Z. Glioma-targeted superparamagnetic iron oxide nanoparticles as drug-carrying vehicles for theranostic effects. *Nanoscale* **2016**, *8*, 14222−14236.

(11) Jacob, J.; Haponiuk, J. T.; Thomas, S. Biopolymer based nanomaterials in drug delivery systems: A review. *Mat. Today Chem.* **2018**, *9*, 43−55.

(12) Baranwal, J.; Barse, B.; Fais, A.; Delogu, G.; Kumar, A. Biopolymer: A Sustainable Material for Food and Medical Applications. *Polymers* **2022**, *14*, 983.

(13) Kumar, S. K.; Saha, P.; Adhikari, J. Recent advances in mechanical properties of biopolymer composites: a review. *Polym. Composites* **2020**, *41*, 32−59.

(14) Salerno, A.; Pascual, C. D. Bio-based polymers, supercritical fluids and tissue engineering. *Process Biochem.* **2015**, *50*, 826−838.

(15) Yimu, L.; Xuling, C.; Jianbo, J.; Lingbing, L.; Guangxi, Z. Redox-responsive nanoparticles based on Chondroitin Sulfate and Docetaxel prodrug for tumor targeted delivery of Docetaxel. *Carbohydr. Polym.* **2021**, *255*, No. 117393.

(16) Ahmad, J.; Ameeduzzafar; Ahmad, M. Z.; Akhter, H. Surface-Engineered Cancer Nanomedicine: Rational Design and Recent Progress. *Curr. Pharm. Des.* **2020**, *26*, 1181−1190.

(17) Akhter, M. H.; Beg, S.; Tarique, M.; Malik, A.; Afaq, S.; Choudhry, H.; Hosawi, S. Receptor-based targeting of engineered nanocarrier against solid tumors: Recent progress and challenges ahead. *Biochim. Biophys. Acta, Gen. Subj.* **2021**, *1865*, No. 129777.

(18) Akhter, M. H.; Rizwanullah, M.; Ahmad, J.; Amin, S.; Ahmad, M. Z.; Minhaj, A.; Mujtaba, A.; Ali, J. Molecular Targets and Nanoparticulate Systems Designed for the Improved Therapeutic Intervention in Glioblastoma Multiforme. *Drug Res.* **2021**, *71*, 122−137.

(19) Letao, X.; Xing, W.; Yun, L.; Guangze, Y.; Robert, J.; Falconer; Chun-Xia, Z. Lipid Nanoparticles for Drug Delivery. *Adv. Nanobiomed. Res.* **2022**, No. 2100109.

(20) Xiong, W.; Guo, Z.; Zeng, B.; Wang, T.; Zeng, X.; Cao, W.; Lian, D. Dacarbazine-Loaded Targeted Polymeric Nanoparticles for Enhancing Malignant Melanoma Therapy. *Front. Bioeng. Biotech.* **2022**, *10*, 84790.

(21) Akhter, M. H.; Amin, S. An investigative approach to the treatment modalities of squamous cell carcinoma. *Curr. Drug Delivery* **2017**, *14*, 597−612.

(22) Akhter, M. H.; Rizwanullah, M.; Ahmad, J.; Ahsan, M. J.; Mujtaba, A.; Amin, S. Nanocarriers in advanced drug targeting: Setting novel paradigm in cancer therapeutics. *Artif. Cells Nanomed. Biotechnol.* **2018**, *46*, 873−884.

(23) Habban Akhter, M.; Madhav, N. S.; Ahmad, J. Epidermal growth factor receptor based active targeting: A paradigm shift towards advance tumor therapy. *Artif. Cells Nanomed. Biotechnol.* **2018**, *46*, 1188−1198.

(24) Khalil, M.; Ely, A. H.; Astari, D.; Eka, S. P.; Yoshitaka, K. Bifunctional folic-conjugated aspartic-modified Fe3O4 nanocarriers for efficient targeted anticancer drug delivery. *RSC Adv.* **2022**, *12*, 4961−4971.

(25) Karim, S.; Akhter, M. H.; Burzangi, A. S.; Alkreathy, H.; Alharthy, B.; Kotta, S.; Md, S.; Rashid, M. A.; Afzal, O.; Altamimi, A.S.A.; Khalilullah, H. Phytosterol-Loaded Surface-Tailored Bioactive-Polymer Nanoparticles for Cancer Treatment: Optimization, In Vitro Cell Viability, Antioxidant Activity, and Stability Studies. *Gels* **2022**, *8*, 219.

(26) Huijuan, S.; Chang, S.; Wenyu, C.; Bingya, Z.; Liwei, L.; Zhenhua, C.; Liang, Z. Folic Acid-Chitosan Conjugated Nanoparticles for Improving Tumor-Targeted Drug Delivery. *BioMed. Res. Int.* **2013**, No. 723158.

(27) Liu, Y.; Kai, L.; Jie, P.; Bin, L.; Si-Shen, F. Folic acid conjugated nanoparticles of mixed lipid monolayer shell and biodegradable polymer core for targeted delivery of Docetaxel. *Biomaterials* **2010**, *31*, 330−338.

(28) Jingjing, Y.; Xiaofeng, L.; Yao, T.; Yufei, Y.; Li, Z.; Qian, Z.; Jiawen, X.; Lun, D.; Yanyan, J. Targeting co-delivery of doxorubicin and gefitinib by biotinylated Au NCs for overcoming multidrug resistance in imaging-guided anticancer therapy. *Colloids Surf., B* **2022**, *217*, No. 112608.

(29) Lakkadwala, S.; dos Santos Rodrigues, B.; Sun, C.; Singh, J. Dual functionalized liposomes for efficient co-delivery of anti-cancer chemotherapeutics for the treatment of glioblastoma. *J. Controlled Release* **2019**, *307*, 247−260.

(30) Zhou, Z.; Jafari, M.; Sriram, V.; Kim, J.; Lee, J.; Ruiz-Torres, S.; Waltz, S. Delayed Sequential Co-Delivery of Gefitinib and Doxorubicin for Targeted Combination Chemotherapy. *Mol. Pharm.* **2017**, *14*, No. 7b00669.

(31) Borbely, J.; Csikósildikó, Z.; Denyicska, S. Stable nano-composition comprising doxorubicin, process for the preparation

https://doi.org/10.1021/acsomega.3c01375
ACS Omega 2023, 8, 28165−28184

thereof, its use and pharmaceutical compositions containing it. WO201415 5142A12014.
(32) Guoliang, L.; Min, W.; Hongyu, H.; Jiannan, L. Doxorubicin-Loaded Tumor-Targeting Peptide-Decorated Polypeptide Nanoparticles for Treating Primary Orthotopic Colon Cancer. *Front Pharm.* **2021**, No. 744811.
(33) Wang, L.; Liang, L.; Shi, S.; Wang, C. Study on the Application of Doxorubicin-Loaded Magnetic Nanodrugs in Targeted Therapy of Liver Cancer. *Appl. Bionics Biomech.* **2022**, *2022*, No. 2756459.
(34) Maemondo, M.; Akira, I.; Kunihiko, K.; Shunichi, S.; Satoshi, O.; Hiroshi, I.; Akihiko, G.; Masao, H.; Hirohisa, Y.; Ichiro, K.; Yuka, F.; Shoji, O.; et al. Gefitinib or Chemotherapy for Non−Small-Cell Lung Cancer with Mutated EGFR. *N. Engl. J. Med.* **2010**, *362*, 2380−2388.
(35) Costanzo, R.; Piccirillo, M. C.; Sandomenico, C.; Carillio, G.; Montanino, A.; Daniele, G.; Giordano, P.; Bryce, J.; De Feo, G.; Di Maio, M.; et al. Gefitinib in non small cell lung cancer. *J. Biomed. Biotech.* **2011**, *2011*, No. 815269.
(36) Makeen, H. A.; Mohan, S.; Al-Kasim, M. A.; Attafi, I. M.; Ahmed, R. A.; Syed, N. K.; Sultan, M. H.; Al-Bratty, M.; Alhazmi, H. A.; Safhi, M. M.; et al. Gefitinib loaded nanostructured lipid carriers: characterization, evaluation and anti-human colon cancer activity in vitro. *Drug Delivery* **2020**, *27*, 622−631.
(37) Lakkadwala, S.; Singh, J. Co-delivery of doxorubicin and erlotinib through liposomal nanoparticles for glioblastoma tumor regression using an in vitro brain tumor model. *Colloids Surf., B* **2019**, *173*, 27−35.
(38) Soni, K.; Mujtaba, A.; Akhter, H.; Zafar, A.; Kohli, K. Optimisation of ethosomal nanogel for topical nano-CUR and sulphoraphane delivery in effective skin cancer therapy. *J. Microencapsul.* **2020**, *37*, 91−108.
(39) Akhter, M. H.; Nomani, S.; Kumar, S. Sonication tailored enhance cytotoxicity of naringenin nanoparticle in pancreatic cancer: Design, optimization, and in vitro studies. *Drug Dev. Ind. Pharm.* **2020**, *46*, 659−672.
(40) Guo, C.; Jeffery, L. Y. Characterizing gold nanoparticles by NMR spectroscopy. *Magn. Reson. Chem.* **2018**, *56*, 1074−1082.
(41) Augustine, R.; Nethi, S. K.; Kalarikkal, N.; et al. Electrospun polycaprolactone (PCL) scaffolds embedded with europium hydroxide nanorods (EHNs) with enhanced vascularization and cell proliferation for tissue engineering applications. *J. Mater. Chem. B* **2017**, *5*, 4660−4672.
(42) Saif, A. A.; Shams, T.; Ahmed, A. M.; Torki, A. Z.; C, K. F. Sugiol Suppresses the Proliferation of Human U87 Glioma Cells via Induction of Apoptosis and Cell Cycle Arrest. *Evidence-Based Complementary Altern. Med.* **2022**, No. 7658899.
(43) Yang, T.; Zang, D-W.; Shan, W.; Guo, A-C.; Wu, J-P.; Wang, Y-J.; Wang, Q. Synthesis and Evaluations of Novel Apocynin Derivatives as Anti-Glioma Agents. *Front. Pharm.* **2019**, *10*, 951.
(44) Akhter, M. H.; Ahmad, A.; Ali, J.; Mohan, G. Formulation and Development of CoQ10-Loaded s-SNEDDS for Enhancement of Oral Bioavailability. *J. Pharm. Innov.* **2014**, *9*, 121−131.
(45) ICH Q5C. Stability testing of biotechnological/biological products. ICH step 4. CPMP/ICH/138/95. European Medicines Agency. July **1996**.
(46) Katas, H.; Hussain, Z.; Awang, S. A. Bovine Serum Albumin-Loaded Chitosan/Dextran Nanoparticles: Preparation and Evaluation of Ex Vivo Colloidal Stability in Serum. *J. Nanomater.* **2013**, No. 536291.
(47) Kausar, H.; Mujeeb, M.; Ahad, A.; Moolakkadath, T.; Aqil, M.; Ahmad, A.; Akhter, M. H. Optimization of ethosomes for topical thymoquinone delivery for the treatment of skin acne. *J. Drug Delivery Sci. Technol.* **2019**, *49*, 177−187.
(48) Alshetaili, A. S. Gefitinib loaded PLGA and chitosan coated PLGA nanoparticles with magnified cytotoxicity against A549 lung cancer cell lines. *Saudi J. Biol. Sci.* **2021**, *28*, 5065−5073.
(49) Sayyed, M. E.; El-Motaleb, M. A.; Ibrahim, I. T.; Rashed, H. M.; Nabarawi, M. A-E.; Ahmed, M. A. Preparation, characterization, and in vivo biodistribution study of intranasal 131I-clonazepam-loaded phospholipid magnesome as a promising brain delivery system. *Eur. J. Pharm. Sci.* **2022**, *169*, No. 106089.
(50) Erdő, F.; Bors, L. A.; Farkas, D.; Bajza, Á.; Gizurarson, S. Evaluation of intranasal delivery route of drug administration for brain targeting. *Brain Res. Bull.* **2018**, *143*, 155−170.
(51) Grassin, D. S.; Buenestado, A.; Naline, E.; Faisy, C.; Blouquit, L. S.; Couderc, L-J.; Guen, M. L.; Fischler, M.; Devillier, P. Intranasal drug delivery: An efficient and non-invasive route for systemic administration: Focus on opioids. *Pharmacol. Ther.* **2012**, *134*, 366−379.
(52) Zottel, A.; Videtic Paska, A.; Jovčevska, I. Nanotechnology Meets Oncology: Nanomaterials in Brain Cancer Research, Diagnosis and Therapy. *Materials* **2019**, *12*, 1588.
(53) Sharma, G.; Modgil, A.; Layek, B.; et al. Cell penetrating peptide tethered bi-ligand liposomes for delivery to brain in vivo: Biodistribution and transfection. *J. Controlled Release* **2013**, *167*, 1−10.
(54) Hosseini, S. M.; Abbasalipourkabir, R.; Jalilian, F. A.; Soleimani, S.; et al. Doxycycline-encapsulated solid lipid nanoparticles as promising tool against Brucella melitensis enclosed in macrophage: a pharmacodynamics study on J774A.1 cell line. *Antimic Resist Infect. Cont.* **2019**, *8*, 62.
(55) Mondal, L.; Mukherjee, B.; Das, K.; Bhattacharya, S.; Dutta, D.; Chakraborty, S.; Pal, M. M.; Gaonkar, R. H.; Debnath, M. C. CD-340 functionalized doxorubicin-loaded nanoparticle induces apoptosis and reduces tumor volume along with drug-related cardiotoxicity in mice. *Int. J. Nanomed.* **2019**, *9*, 8073−8094.
(56) Mac, D. J. A.; Langova, V.; Bailey, D.; Pattison, S. T.; Pattison, S. L.; Christensen, N.; Armstrong, L. R.; Brahmbhatt, V. N.; Smolarczyk, K.; Harrison, M. T. Targeted Doxorubicin Delivery to Brain Tumors via Minicells: Proof of Principle Using Dogs with Spontaneously Occurring Tumors as a Model. *PLoS One* **2016**, *11*, No. e0151832.
(57) Liu, Y.; Zhang, Y.; Feng, G.; Niu, Q.; Xu, S.; Yan, Y.; Li, S.; Jing, M. Comparison of effectiveness and adverse effects of gefitinib, erlotinib and icotinib among patients with non small cell lung cancer: A network meta analysis. *Exp. Ther. Med.* **2017**, *14*, 4017−4032.
(58) Li, X.; Wang, J.; Li, S.; Liu, Z.; Zheng, Z.; Zhang, Y. Development and Evaluation of Multifunctional Poly(Lactic-co-glycolic acid) Nanoparticles Embedded in Carboxymethyl β-Glucan Porous Microcapsules as a Novel Drug Delivery System for Gefitinib. *Pharmaceutics* **2019**, *11*, 469.
(59) Liu, Y.; Kai, L.; Jie, P.; Bin, L.; S, F. Folic acid conjugated nanoparticles of mixed lipid monolayer shell and biodegradable polymer core for targeted delivery of Docetaxel. *Biomaterials* **2010**, *31*, 330−338.
(60) Ullah, S.; Azad, A. K.; Nawaz, A.; Shah, K. U.; Iqbal, M.; Albadrani, G. M.; Al-Joufi, F. A.; Sayed, A. A.; Abdel-Daim, M. M. 5-Fluorouracil-Loaded Folic-Acid-Fabricated Chitosan Nanoparticles for Site-Targeted Drug Delivery Cargo. *Polymers* **2022**, *14*, No. 35631891.
(61) Emwas, A.-H.; Szczepski, K.; Poulson, B. G.; Chandra, K.; McKay, R. T.; Dhahri, M.; Alahmari, F.; Jaremko, L.; Lachowicz, J. I.; Jaremko, M. NMR as a "Gold Standard" Method in Drug Design and Discovery. *Molecules* **2020**, *25*, 4597.
(62) Tzeyung, A. S.; Md, S.; Bhattamisra, S. K.; et al. Fabrication, Optimization, and Evaluation of Rotigotine-Loaded Chitosan Nanoparticles for Nose-To-Brain Delivery. *Pharmaceutics* **2019**, *11*, 26.
(63) Chen, Y.; Xiaoxia, L.; Hong, X.; Jinpeng, X.; Bo, L.; Xiaoyan, C.; Yong, W.; Du, C.; Xintao, S. Reduction and pH dual-sensitive nanovesicles co-delivering doxorubicin and gefitinib for effective tumor therapy. *RSC Adv.* **2018**, *8*, 2082−2209.
(64) Pan, D.; Vargas; M, O.; Zern, B.; et al. The Effect of Polymeric Nanoparticles on Biocompatibility of Carrier Red Blood Cells. *PLoS One* **2016**, *11*, No. e0152074.
(65) Ghosh, R.; Mondal, S.; Adhikari, A.; Ahmed, S. A.; Alsantali, R. I.; Abdelrahman, S.; Khder, A. S.; Altass, H. M.; Moussa, Z.; Das, R.; Bhattacharyya, M.; Pal, S. K. Oral drug delivery using a polymeric nanocarrier: chitosan nanoparticles in the delivery of rifampicin. *Mater. Adv.* **2022**, *3*, 4622−4628.
(66) Md, S.; Alhakamy, N. A.; Neamatallah, T.; Alshehri, S.; Mujtaba, M. A.; Riadi, Y.; Radhakrishnan, A. K.; Khalilullah, H.; Gupta, M.; Akhter, M. H. Development, Characterization, and Evaluation of α-Mangostin-Loaded Polymeric Nanoparticle Gel for Topical Therapy in Skin Cancer. *Gels* **2021**, *7*, 230.

https://doi.org/10.1021/acsomega.3c01375
ACS Omega 2023, 8, 28165−28184

(67) Li, S.; Xu, Z.; Alrobaian, M.; Afzal, O.; Kazmi, I.; Almalki, W. H.; Altamimi, A.S.A.; Al-Abbasi, F. A.; Alharbi, K. S.; Altowayan, W. M.; Singh, T.; Akhter, M. H.; Gupta, M.; Rahman, M.; Beg, S. EGF-functionalized lipid−polymer hybrid nanoparticles of 5-fluorouracil and sulforaphane with enhanced bioavailability and anticancer activity against colon carcinoma. *Biotechnol. Appl. Biochem.* **2021**, 2205−2221.
(68) Ali, H.; Kilic, G.; Vincent, K.; Motamedi, M.; Rytting, E. Nanomedicine for Uterine Leiomyoma Therapy. *Therap. Delivery* **2013**, *4*, 161−175.
(69) Gheorghita, R.; Norocel, L.; Filip, R.; Dimian, M.; Covasa, M. Applications of Biopolymers for Drugs and Probiotics Delivery. *Polymers* **2021**, *13*, 2729.
(70) Xu, H.; Rahimpour, S.; Nesvick, C.; et al. Activation of hypoxia signaling induces phenotypic transformation of glioma cells: Implications for bevacizumab antiangiogenic therapy. *Oncotarget* **2015**, *6*, 11882−11893.
(71) Kumar, S.; Besra, S. E. The Growth Suppressing Activity of Spathodea Campanulata Bark on C6 & U87mg Involve Induction of Apoptosis and Cell Cycle Arrest. *World J. Pharm. Res.* **2020**, *9*, 2517.
(72) Chou, T. C. Drug combination studies and their synergy quantification using the Chou-Talalay method. *Cancer Res.* **2010**, *70*, 440−446.
(73) Zhou, Z.; Jafari, M.; Sriram, V.; Kim, J.; Lee, J-Y.; Ruiz-Torres, S.; Waltz, S. Delayed Sequential Co-Delivery of Gefitinib and Doxorubicin for Targeted Combination Chemotherapy. *Mol. Pharm.* **2017**, *14*, 4551−4559.
(74) Xu, C.; Song, R.; Lu, P.; Chen, J-c.; Zhou, Y-q.; Shen, G.; Jiang, M-j.; Zhang, W. pH-triggered charge-reversal and redox-sensitive drug release polymer micelles co-deliver doxorubicin and triptolide for prostate tumor therapy. *Int. J. Nanomed.* **2018**, *13*, 7229−7249.
(75) Farheen, M.; Akhter, M. H.; Chitme, H.; Akhter, M. S.; Tabassum, F.; Jaremko, M.; Emwas, A.-H. Harnessing Folate-Functionalized Nasal Delivery of Dox−Erlo-Loaded Biopolymeric Nanoparticles in Cancer Treatment: Development, Optimization, Characterization, and Biodistribution Analysis. *Pharmaceuticals* **2023**, *16*, No. 207.
(76) Palanikumar, L.; Al-Hosani, S.; Kalmouni, M.; et al. pH-responsive high stability polymeric nanoparticles for targeted delivery of anticancer therapeutics. *Commun. Biol.* **2020**, *3*, No. 95.

https://doi.org/10.1021/acsomega.3c01375
ACS Omega 2023, 8, 28165−28184